Swiss Journal of Geosciences (2019) 112:101–120
https://doi.org/10.1007/s00015-018-0322-7

Post-Variscan metamorphism in the Apuseni and Rodna Mountains (Romania): evidence from Sm–Nd garnet and U–Th–Pb monazite dating

Martin Kaspar Reiser[1,3] · Gavril Săbău[2] · Elena Negulescu[2] · Ralf Schuster[3] · Peter Tropper[4] · Bernhard Fügenschuh[1]

Received: 1 May 2018 / Accepted: 24 September 2018 / Published online: 12 October 2018

Abstract
The Tisza and Dacia mega-units constitute a central part of the Alps-Carpathians-Dinarides orogenic system. Polyphase medium-grade metamorphism observed in mineral assemblages from the crystalline basement is often correlated with Variscan and pre-Variscan events. However, a mid-Cretaceous Sm–Nd garnet age (103.6 ± 1.8 Ma) from the Apuseni Mountains is at odds with this interpretation. Electron-microprobe U-Th–Pb dating of monazite in samples from the Apuseni Mountains, the Rodna Mountains, as well as the Şimleu Silvaniei, Ticău and Preluca inselbergs revealed a complex pattern of Alpine and pre-Alpine age clusters. Pre-Variscan and Variscan ages were obtained from the core of zoned monazite grains and from samples that apparently escaped Alpine overprinting. Relic monazite in the latter is often replaced by rhabdophane and/or surrounded by allanite coronas. Permian to Early Triassic monazite ages correlate with the intrusion of granitic melts and pegmatites. Early Cretaceous ages from rims of chemically zoned grains and from monazite inclusions in garnet, biotite and staurolite represent newly formed metamorphic grains that crystallized on the prograde path during Alpine metamorphism. Petrographic observations of prograde allanite breakdown reactions, Sm–Nd garnet analyses and thermobaric estimates (500–550 °C/5–8 kbar) from parts of the Tisza and Dacia mega-units constrain medium-grade conditions during Early Cretaceous times. Exclusively mid-Cretaceous monazite ages from the inselbergs and the Rebra-Unit of the Rodna Mountains, allow extending the Alpine prograde overprint across the Transylvanian basin. Together with other studies from the basement of the Pannonian basin, this implies that the Dacia Mega-Unit and parts of the Tisza Mega-Unit experienced a medium-grade metamorphic overprint and synkinematic garnet-growth during late Early Cretaceous times. The Alpine prograde medium-grade overprint is pronounced in the contact zone between the Tisza and Dacia mega-units and forms a continuous belt with the Cretaceous metamorphic imprint in the Eastern Alps, when back-rotated to its original position during the Cretaceous.

Keywords Medium-grade metamorphism · Tisza · Dacia · Cretaceous · Transylvania

1 Introduction

During the last few years, significant advances were made in understanding the tectonometamorphic evolution of the Alps-Carpathians-Dinarides orogenic system during the

Editorial handling: V. Cvetković & S. Schmid.

Electronic supplementary material The online version of this article (https://doi.org/10.1007/s00015-018-0322-7) contains supplementary material, which is available to authorized users.

✉ Gavril Săbău
g_sabau@yahoo.co.uk

[1] Institut für Geologie, Universität Innsbruck, Innrain 52f, 6020 Innsbruck, Austria

[2] Geological Institute of Romania, Caransebeş 1, Sector 1, Bucharest, Romania

[3] Present Address: Geologische Bundesanstalt, Neulinggasse 38, 1030 Vienna, Austria

[4] Institut für Mineralogie und Petrographie, Universität Innsbruck, Innrain 52f, 6020 Innsbruck, Austria

Cretaceous, based on new information (e.g. Necea 2010; Gröger et al. 2013; Balen et al. 2013, 2017; Antić et al. 2016; van Gelder et al. 2015; Erak et al. 2016; Reiser et al. 2017a). However, some authors referred and still refer to the Alpine (i.e. Cretaceous-age) metamorphic evolution of the Tisza and Dacia mega-units as being retrogressive, taking place under low-grade conditions, while medium-grade conditions are exclusively attributed to pre-Variscan and Variscan events (e.g. Balintoni et al. 1983; Pană et al. 2002; Munteanu and Tatu 2003; Balintoni et al. 2010, 2014). Several publications (e.g. Dallmeyer et al. 1999; Radu 2003; Gröger et al. 2013) challenged this interpretation, emphasising the importance of Alpine overprint. However, correlations of the metamorphic and structural evolution between the ALCAPA, Tisza and Dacia mega-units are still problematic because of (1) poly-metamorphic pre-Alpine and Alpine metamorphic overprint under similar P–T conditions and (2) extensive Cenozoic cover of the Pannonian and Transylvanian basins fill hiding bedrocks (cf. outlines of these basins marked in Fig. 1).

Thus, to evaluate timing and metamorphic conditions of post-Variscan (i.e. Alpine) metamorphism, samples from the Apuseni Mountains (Mts.) were investigated using U–Th–Pb dating of monazites, Sm–Nd garnet dating and thermobarometric analyses. Samples from the Transylvanian inselbergs (i.e. Şimleu Silvaniei, Ţicău and Preluca Inselbergs) and from the Rodna Mts. (Fig. 1) were also analyzed using U–Th–Pb dating of monazite. Monazite-Allanite reactions, chemical information and textural observations provide information on the prograde evolution in metapelites (e.g. Smith and Barreiro 1990; Wing et al. 2003; Kohn and Malloy 2004; Janots et al. 2007; Janots et al. 2008; Spear 2010). Together with U–Th–Pb dating,

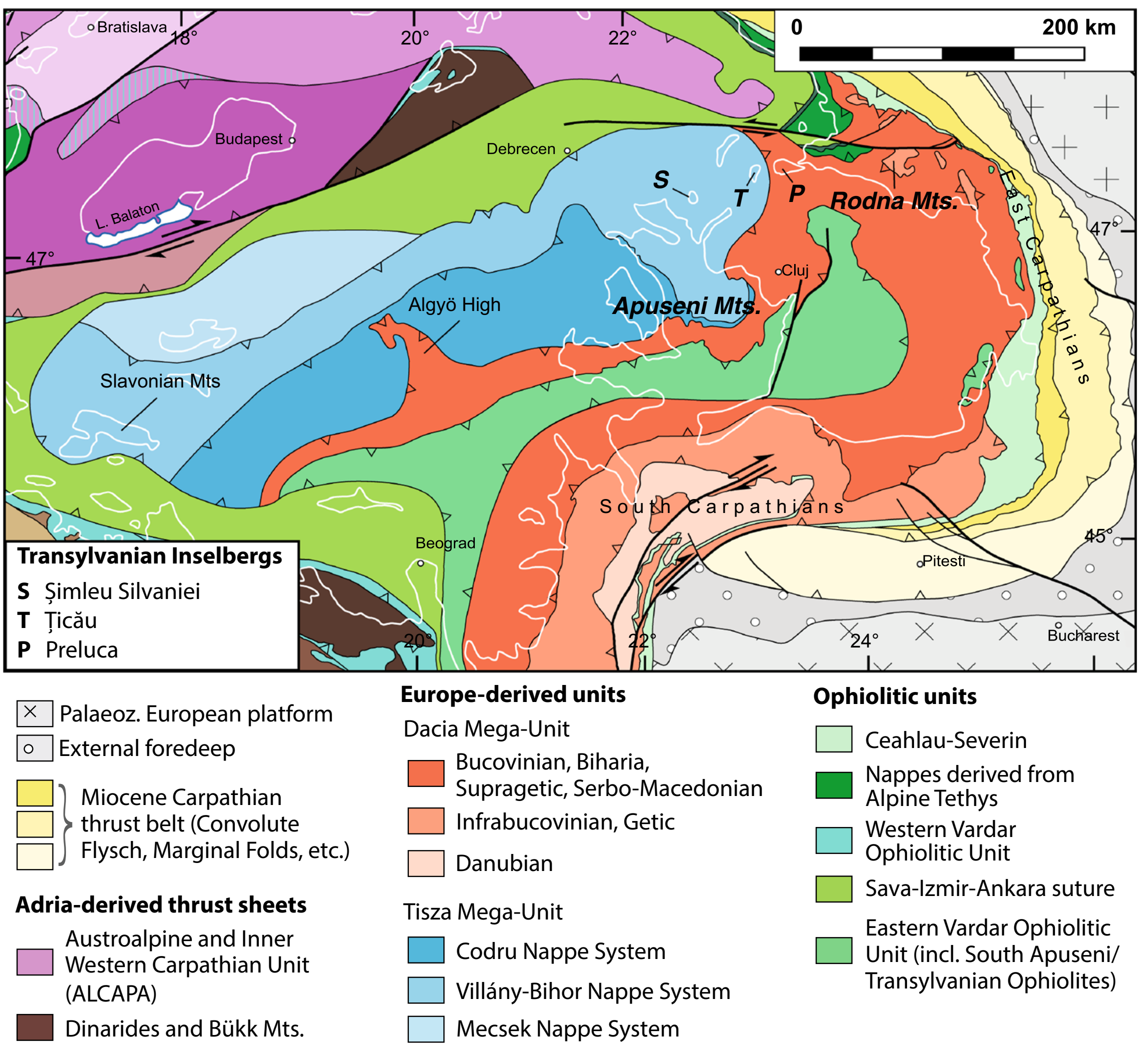

Fig. 1 Map showing the major tectonic units of the Alps-Carpathian-Dinaride system of orogens modified from Schmid et al. (2008). The Cenozoic cover sediments of the Pannonian and Transylvanian basins are not shown, but white lines delineate their extent, covering much of the area around isolated inselbergs

thermobaric analyses and Sm–Nd garnet dating, tight constraints on the metamorphic evolution are obtained. Following earlier correlations of geochronological data across the Transylvanian basin (Zincenco et al. 1990; Strutinski et al. 2006), this study aims to provide new constraints and correlations on the metamorphic evolution of the Tisza and Dacia mega-units including that of isolated Transylvanian inselbergs whose attribution is uncertain.

2 Geological setting

During the Early Mesozoic, the Tisza and Dacia mega-units were located north of the northern branch of Neotethys, forming the southern margin of the European Plate and located east of the ALCAPA Mega-Unit (cf. Haas and Péró 2004; Csontos and Vörös 2004; Schmid et al. 2008; Pozsgai et al. 2017). Their present-day arrangement is the consequence of large clockwise (Tisza-Dacia) and anticlockwise (ALCAPA) rotations during the Miocene (e.g. Balla 1987; Pătraşcu et al. 1994, Márton 2000; Márton and Fodor 2003; Lorinczi and Houseman 2010). Both Tisza and Dacia consist of a Variscan polymetamorphic basement (Pană et al. 2002; Balintoni et al. 2009b, Balintoni et al. 2010) with Late Carboniferous and Permian granitic intrusions (Pană and Balintoni 2000; Balintoni et al. 2009a). Variscan imbrication of reworked and juvenile basement units is indicated (Negulescu et al. 2018). Late Palaeozoic metasediments and Mesozoic sequences of variable thickness are locally preserved (e.g. Mârza 1965; Bleahu et al. 1981; Haas and Péró 2004; Reiser et al. 2017b). The present study uses the tectonic scheme of Schmid et al. (2008), which is partly based on Săndulescu (1984) concerning our study area (Figs. 1 and 2). The two mega-units are largely covered by Cenozoic sediments, but several small inselbergs (i.e. Şimleu Silvaniei, Ţicău and Preluca Inselbergs) represent a fragmentary connection of basement between the larger exposures in the Apuseni and Rodna Mts. (Fig.1).

2.1 Dacia Mega-Unit

The Dacia Mega-Unit comprises the Biharia Nappe System in the Apuseni Mts., the Rodna Mts. and the Preluca Inselberg (cf. Figs 1 and 2a). In turn, the Biharia Nappe System consists of several Alpine thrust sheets, that are from bottom to top, the Biharia Nappe sensu stricto (s.str.), the Baia de Arieş Nappe and the Vidolm Nappe (Fig. 2; e.g. Mârza 1965; Ianovici et al. 1976; Balintoni 1982; Săndulescu 1984; Balintoni and Iancu 1986; Balintoni 1994; Balintoni et al. 1996; Dallmeyer et al. 1999; Kounov and Schmid 2013). The Rodna Mts. (cf. Fig. 2b) comprise two distinct nappes: a structurally higher Rebra Unit correlated with the Subbucovinian Nappe in the East Carpathians, and a lower Bretila Unit attributed to the Infrabucovinian Nappe (Balintoni et al. 1997; Mosonyi 1999; Gröger 2006; Tischler et al. 2008; Schmid et al. 2008; Gröger et al. 2008, 2013). Some authors correlate the Rebra Unit in the Rodna Mts. with the Baia de Arieş Nappe (e.g. Pană et al. 2002; Balintoni et al. 2009b), while the Bretila Unit is correlated with the Bihor Unit of the Apuseni Mts. (Balintoni et al. 2014); Fig. 1 attributes both to the Dacia Mega-Unit. All these units share a complex metamorphic evolution during three discrete events: two amphibolite-facies overprints of similar grade, followed by greenschist-facies retrogression (Balintoni and Gheuca 1977; Balintoni et al. 1983; Balintoni and Iancu 1986; Dimitrescu 1994; Udubaşa et al. 1996; Balintoni et al. 1997; Radu 1997; Denuţ 1998; Radu 2003). Furthermore, a Permo-Triassic metamorphic event is reported from the Rodna Mts. (Culshaw et al. 2012; Mosonyi and Kristály 2014). The Late Jurassic emplacement ($\sim$ 153 Ma; Nicolae et al. 1992; Bortolotti et al. 2004; Bucur and Săsăran 2005; Zimmerman et al. 2008; Gallhofer et al. 2017) of the South Apuseni-Transylvanian ophiolite (part of the Eastern Vardar Ophiolitic Unit) on top of the Biharia Nappe System marks the onset of the Alpine tectonic evolution in the study area (D0 sensu Reiser et al. 2017a). Subsequent NE-directed nappe stacking during Early Cretaceous times (D1: $\sim$ 135–110 Ma) is reported from both the Apuseni Mts. (Reiser et al. 2017a) and the Rodna Mts. (Gröger et al. 2013).

2.2 Tisza Mega-Unit

The Tisza Mega-Unit consists of three main nappe systems of Alpine origin that are, from bottom to top, the Mecsek, Villány-Bihor (Bihor) and Codru nappe systems (Fig. 1; Kovaćs et al. 1989; Haas et al. 1995; Haas and Péró 2004; Szederkényi et al. 2012; Haas 2013) whereby the Mecsek Nappe System is not exposed in our study area (Fig. 2). The Codru Nappe System predominantly consists of non-metamorphic, Mesozoic sediments in the western part of Fig. 2a (Bleahu et al. 1981; Haas and Péró 2004); Codru basement outcrops are located in the Codru Mountains and within a thin basement sliver separating the Bihor Unit (Tisza) from the Biharia Nappe System (Dacia; see easternmost part of Fig. 2a). The Bihor Unit consists of a metamorphic basement (paragneiss, orthogneiss, micaschist and subordinate amphibolite, referred to as Someş Series; Bleahu and Dimitrescu 1957) and a Permo-Mesozoic cover (only preserved in western parts of the Apuseni Mts.; Fig. 2a). The metamorphic basement was intruded by a Permian pluton (Muntele Mare; Balintoni et al. 2009a) and Triassic pegmatites (Anton 1999). Hârtopanu and Hârtopanu (1986) recognized three metamorphic events in the basement of the Bihor Unit: a primary Grt–St–Ky (Whitney and Evans 2010) mineral assemblage overprinted by a second metamorphic event, evidenced through syn-

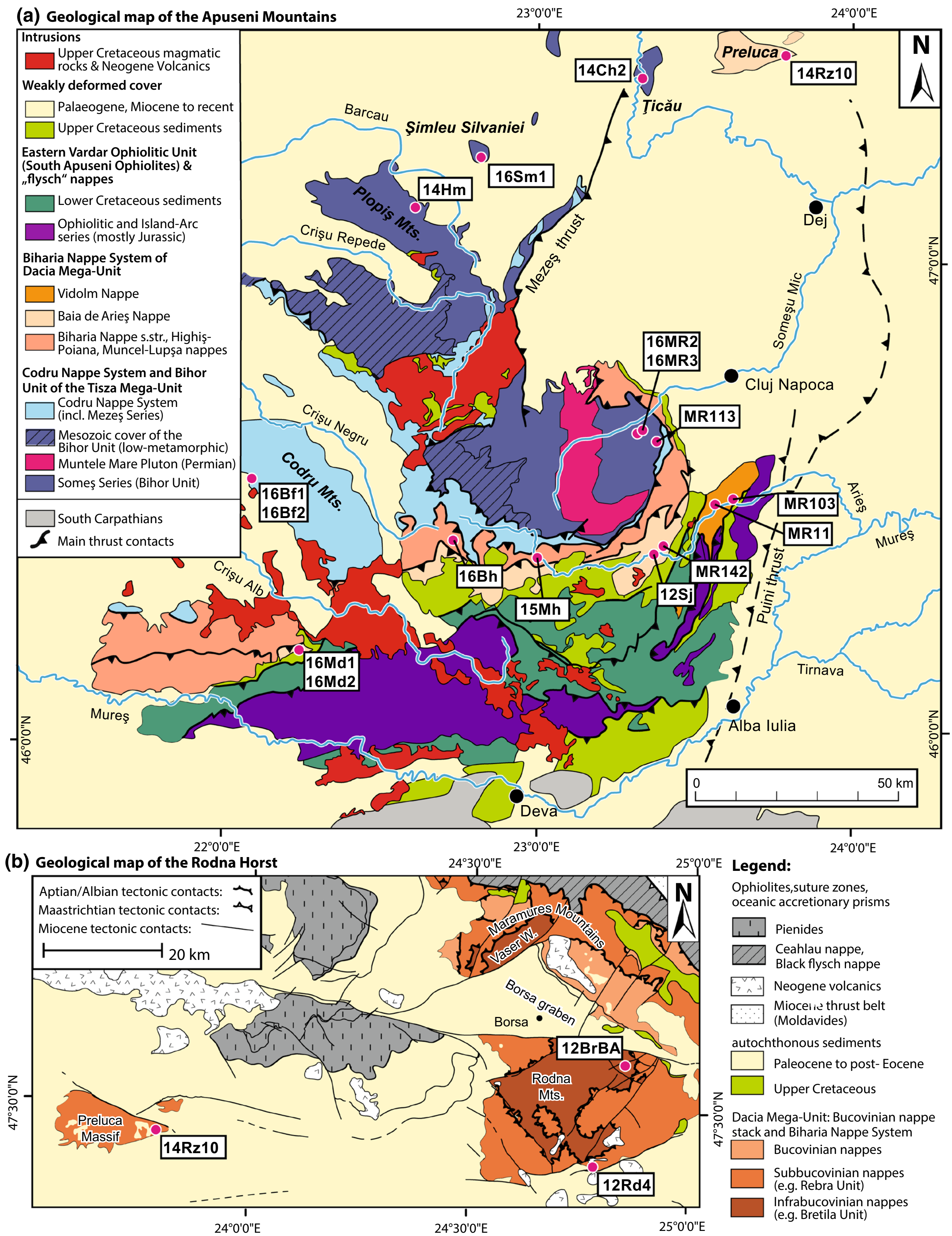
(a) Geological map of the Apuseni Mountains
Intrusions
Upper Cretaceous magmatic rocks & Neogene Volcanics
Weakly deformed cover
Palaeogene, Miocene to recent
Upper Cretaceous sediments
Eastern Vardar Ophiolitic Unit (South Apuseni Ophiolites) & „flysch" nappes
Lower Cretaceous sediments
Ophiolitic and Island-Arc series (mostly Jurassic)
Biharia Nappe System of Dacia Mega-Unit
Vidolm Nappe
Baia de Arieş Nappe
Biharia Nappe s.str., Highiş-Poiana, Muncel-Lupşa nappes
Codru Nappe System and Bihor Unit of the Tisza Mega-Unit
Codru Nappe System (incl. Mezeş Series)
Mesozoic cover of the Bihor Unit (low-metamorphic)
Muntele Mare Pluton (Permian)
Someş Series (Bihor Unit)
South Carpathians
Main thrust contacts
23°0'0"E
24°0'0"E
22°0'0"E
47°0'0"N
46°0'0"N
N
Preluca
14Rz10
14Ch2
Ţicău
Barcau
Şimleu Silvaniei
16Sm1
14Hm
Plopiş Mts.
Crişu Repede
Mezeş thrust
Dej
Someşu Mic
16MR2
16MR3
Cluj Napoca
MR113
Crişu Negru
Codru Mts.
16Bf1
16Bf2
MR103
MR11
Arieş
Mureş
16Bh
MR142
12Sj
15Mh
Puini thrust
Crişu Alb
16Md1
16Md2
Tirnava
Alba Iulia
Mureş
Deva
0
50 km
(b) Geological map of the Rodna Horst
Aptian/Albian tectonic contacts:
Maastrichtian tectonic contacts:
Miocene tectonic contacts:
20 km
24°30'0"E
25°0'0"E
24°0'0"E
47°30'0"N
N
Maramureş Mountains
Vaser W.
Borsa graben
Borsa
12BrBA
Rodna Mts.
Preluca Massif
14Rz10
12Rd4
Legend:
Ophiolites,suture zones, oceanic accretionary prisms
Pienides
Ceahlau nappe, Black flysch nappe
Neogene volcanics
Miocene thrust belt (Moldavides)
autochthonous sediments
Paleocene to post- Eocene
Upper Cretaceous
Dacia Mega-Unit: Bucovinian nappe stack and Biharia Nappe System
Bucovinian nappes
Subbucovinian nappes (e.g. Rebra Unit)
Infrabucovinian nappes (e.g. Bretila Unit)

◀ **Fig. 2** Tectonic maps illustrating the sample locations in **a** the Apuseni Mts. and **b** the Rodna Mts. Modified from Kounov and Schmid (2013) and Tischler et al. (2007), respectively

kinematic garnet growth and static overgrowth of staurolite and kyanite. Sillimanite nodules nucleating on kyanite formed during the first metamorphic event were interpreted to relate to post peak-metamorphic uplift and exhumation. A third, low-grade metamorphic overprint, intersecting with the isograds of the former medium-grade events is correlated with a pervasive greenschist-facies overprint visible in all tectonic units of the Apuseni Mts. (Dimitrescu 1966; Hârtopanu et al. 1982). The timing of these events is not well constrained, but several studies report indications for an Early Cretaceous prograde overprint in both Mesozoic sediments and pre-Triassic basement beneath the sediments of the Pannonian Basin (e.g. Árkai et al. 1998, 2000; Árkai 2001; Horváth and Árkai 2002; Lelkes-Felvári et al. 2003, 2005). The present-day, SE-dipping and NW-directed nappe-stack of the Apuseni Mts. with the Bihor Unit as the lowest unit, overlain by the Codru Nappe System and the Biharia Nappe System was found to be of mid-Cretaceous age by combining sedimentary and geochronological data (D2: 110–90 Ma; Reiser et al. 2017a). Significant east-directed exhumation (D3) and associated retrograde overprinting during Late Cretaceous times was shown for the Apuseni Mountains (Reiser et al. 2017a) and the Rodna Mts. (Gröger 2006; Gröger et al. 2013; Mosonyi and Kristály 2014). Deposition of Late Cretaceous, syn- to post-tectonic sediments in the hanging wall of detachments (Schuller 2004; Gröger et al. 2008; Schuller et al. 2009; Kounov and Schmid 2013) constrains the surface-near position of the basement units.

The Şimleu Silvaniei and Ţicău inselbergs are generally attributed to the Tisza Mega-Unit (Dimitrescu 1963; Zincenco et al. 1990; Kalmár 1994; Kalmár and Kovaćs-Pálffy 1996, Schmid et al. 2008), although different correlations for the latter are also discussed (Săndulescu 1984; Zincenco et al. 1990). Both these inselbergs expose micaschist, paragneiss, pegmatite and subordinate orthogneiss which locally show strong mylonitization. Zoned garnet (Alm) and the observation of distinct medium-grade mineral assemblages indicate a polyphase metamorphic evolution (Kalmár 1996; Kalmár and Kovaćs-Pálffy 1996; Radu 2003).

3 Sample description

19 samples from the Apuseni and Rodna Mts., the Şimleu Silvaniei, Ţicău and Preluca inselbergs were investigated by the present study. Sample localities and general information are given in Fig. 2 and Table 1. Relevant thin section photographs and back-scattered electron (BSE) images are shown in Figs. 3, 4 and 5. Detailed descriptions of individual samples and references to thin section images are provided in Online Resource 1.

4 Methods of investigation

Sample preparation for Sm–Nd analyses followed standard separation procedures. Details concerning the methodology followed for Sm-Nd dating of garnet, U–Th–Pb dating of monazite, and PT-analyses are provided in Online Resource 1.

5 Results

5.1 Thermobarometry

P–T conditions (Table 2) were calculated from mineral equilibria in seven samples from pelitic schist and paragneiss. Where possible, the results were compared with thermal estimates from Ti-in-biotite calculations (Henry and Guidotti 2002; Henry et al. 2005). The samples from the Apuseni Mts. yield temperatures of ~ 550 °C and geobarometric conditions generally range between 0.5 and 0.8 GPa. Unfortunately, it was not possible to calculate geobarometric conditions for sample MR142 due to the lack of plagioclase in this sample. Altogether, the dataset concurs with medium-grade conditions (epidote–amphibolite or amphibolite facies), except for sample MR11 from the Vidolm nappe that yields significantly higher estimates indicating uppermost amphibolite-facies conditions (~ 1.1 GPa and 635 ± 80 °C).

5.2 Garnet zoning

Data of representative electron microprobe analyses, end-member compositions and element distribution mapping of garnet are provided in Online Resources 3 and 4. Zoning profiles (Fig. 6) of the analysed garnet minerals apparently indicate continuous, single-phase growth. However, optical zoning with inclusion-rich cores and inclusion-free rims can be observed in several samples, e.g. MR113 from the Bihor Unit (Figs. 3, 6 and Online Resource 4); yet, the transitions are not always sharp. The garnet is predominantly almandine-rich with a higher spessartine and grossular component in the core. The fact that Fe and Mg contents increase from core to rim, while Mn content decreases, indicates prograde zoning (Fig. 6). The absence of retrograde indicators (Tuccillo et al. 1990) argues for rapid exhumation and minimal residence time at peak *P–T* conditions. A second, small and inclusion free garnet population observed in samples MR113 (Bihor

Table 1 Summary of investigated samples

Sample	Latitude	Longitude	Tectonic Unit	Lithology	Assemblage	P and REE minerals
MR103	46°30'16.85″	23°34'45.8″	Vidolm Nappe	Paragneiss	Qz–Ms–Grt–Pl–Bt–Chl	Mnz–Xtm–Ap–Aln
MR11	46°30′0.23″	23°31′44.59″	Vidolm Nappe	Paragneiss	Qz–Bt–Ms–Pl–Grt–Chl–Ky–St–Ilm	Mnz–Xtm–Ap–Aln
MR15	46°27′6.26″	23°24′31.37″	Baia de Arieş N.	Mica Schist	Qz–Ms–Bt–Grt–Pl–Chl–Zr–Ilm	Ap–Aln
MR61	46°25′4.58″	23°17′5.63″	Baia de Arieş N.	Sericite Schist	Qz–Ms–Grt–Chl–Zr–Px–Ilm	Ap
MR142	46°24′40.25″	23°23′4.42″	Baia de Arieş N.	Grt–St–Mica Schist	Qz–Bio–Pl–St–Grt–Ky–Sil–Mus	Mnz–Xtm–Ap–Aln–Thr
12Sj	46°24′1.42″	23°22′32.90″	Baia de Arieş N.	Grt–St–Mica Schist	Qz–Bio–Pl–St–Grt–Ky–Sil–Mus	Mnz–Xtm–Ap–Aln–Thr
16Md1	46°11′26.44″	22°15′50.54″	Baia de Arieş N.	Gneiss	Qz–Ms–Grt–Pl	Mnz–Aln–Thr
16Md2	46°11′40″	22°16′39″	Baia de Arieş N.	Mica Schist	Qz–Ms–Grt–Pl	Mnz–Aln–Thr
16Bh2	46°26′13.80″	22°41′41.40″	Biharia N. s.str.	Mica Schist	Qz–Ms–Pl	Mnz–Aln–(Y)Ep
16Bf1	46°34′59.61″	22° 6′15.93″	Codru Unit	Gneiss	Qz–Ms–Chl–Zr–Rt–Ilm	Rhb–Xtm–Cheralite–Mnz
16Bf2	46°34′25.92″	22° 5′25.34″	Codru Unit	Metagranite	Qz–Ms–Chl–Zr–Rt–Ilm	Mnz–(Th, REE)Ap–Aln–Thr
15Mh	46°22′59.24″	23° 0′6.25″	Codru Unit	Schist	Qz–Ms–Ab–Cc–Zr	Rhb–Xtm–REEcarb.–Mnz
MR32	46°32′53.86″	23°20′24.14″	Bihor Unit—Someş	Mica Schist	Qz–Grt–Ms–Bt–Ep–Zr–Ilm	Mnz–Xtm–Ap–Aln
MR113	46°38′14.28″	23°21′50.47″	Bihor Unit – Someş	Grt–Mica Schist	Ms–Qz–Grt–Fsp–Bt–Ep–St–Chl–Py	Mnz–Xtm(?)–Ap–Aln
16MR2	46°39′47.14″	23°18′31.79″	Bihor Unit—Someş	Grt–Mica Schist	Ms–Qz–Grt–Fsp–Bt–St–Chl–Rt–Ilm	Mnz–Rhb
16MR3	46°40′11.94″	23°19′40.87″	Bihor Unit—Someş	Grt–Mica Schist	Ms–Qz–Grt–Fsp–Bt–St–Chl–Rt–Ilm	Mnz–Xtm–Ap–Aln
16Sm1	47°14′16.78″	22°47′58.99″	Bihor Unit—Someş	Gneiss	Qz–Ms–Ilm–Ep–Zr	Mnz–Xtm–Ap
14Hm	47°08′46″	22°34′02″	Bihor Unit–Someş	Schist	Ms–Chl–Bt–Pl–Grt–Zr–Py	Mnz–Xtm–Rhb
14Ch2	47°25′10.04″	23°18′59.86″	Tiholţ	Grt–Mica Schist	Qz–Grt–Ms–Bt–Chl–Ilm–Zr–Ky	large Mnz
14Rz10	47°27′27.23″	23°47′31.32″	Răzoare	Grt–Mica Schist	Qz–Grt–Ms–Ap–Zr–Rt–Ilm–Ky	large Mnz
12Rd4	47°25′46.29″	24°48′50.82″	Subbucovin.–Rebra	Grt–St–Mica Schist	Qz–Ms–Bt–St–Grt–Pl–Rt	Mnz–Rhb
12BrBA	47°35′30″	24°51′30″	Infrabucovin.–Bretila	Grt–Mica Schist	Ms–Qz–Chl–Grt–Pl–Ph–Ilm–Rt	Mnz–Rhb–Ap–Aln–Ep

Abbreviations of mineral names are given according to Whitney and Evans (2010)

Unit) and MR142 (Baia de Arieş Nappe) shows a chemical composition similar to that of the rims of the larger grains (Fig. 6).

5.3 Results of ^{147}Sm/^{144}Nd analyses

The results of ^{147}Sm/^{144}Nd measurements from samples MR113 (Bihor Unit; Tisza Mega-Unit) and MR142 (Baia de Arieş Nappe; Dacia Mega-Unit) are given in Fig. 7 and in Online Resource 2. Chemical mappings as well as zoning profiles were carried out to check on single vs. polyphase garnet growth in both these samples. Garnet in sample MR113 shows many inclusions in the core and an inclusion-free rim (Figs. 3 and 6). The inclusion-rich core of the garnet was avoided/minimized by careful hand-picking of clean and clear garnet grains. The whole rock of sample MR113 is characterized by an $\varepsilon_{Nd}(0)$ (CHUR) of -15.4, a ^{147}Sm/^{144}Nd ratio of ~ 0.10, and by Sm (11.47 ppm) and Nd (65.23 ppm) contents that are within the range typical for metapelites (McCulloch and Wasserburg 1978). The two investigated garnet fractions show variable Sm concentrations of 3.3–4.3 ppm and differing Nd concentrations of 3.2 and 10.0 ppm. ^{147}Sm/^{144}Nd ratios are 0.6 and 0.3, respectively. The resulting age is 103.6 ± 1.8 Ma for sample MR113 (Fig. 7). The closure temperature (T_C) for the Sm–Nd system in garnet ranges from 600–820 °C (Hölzl et al. 1991; Mezger et al. 1992; Thöni 2002; Thöni et al. 2008; Dutch and Hand 2010),

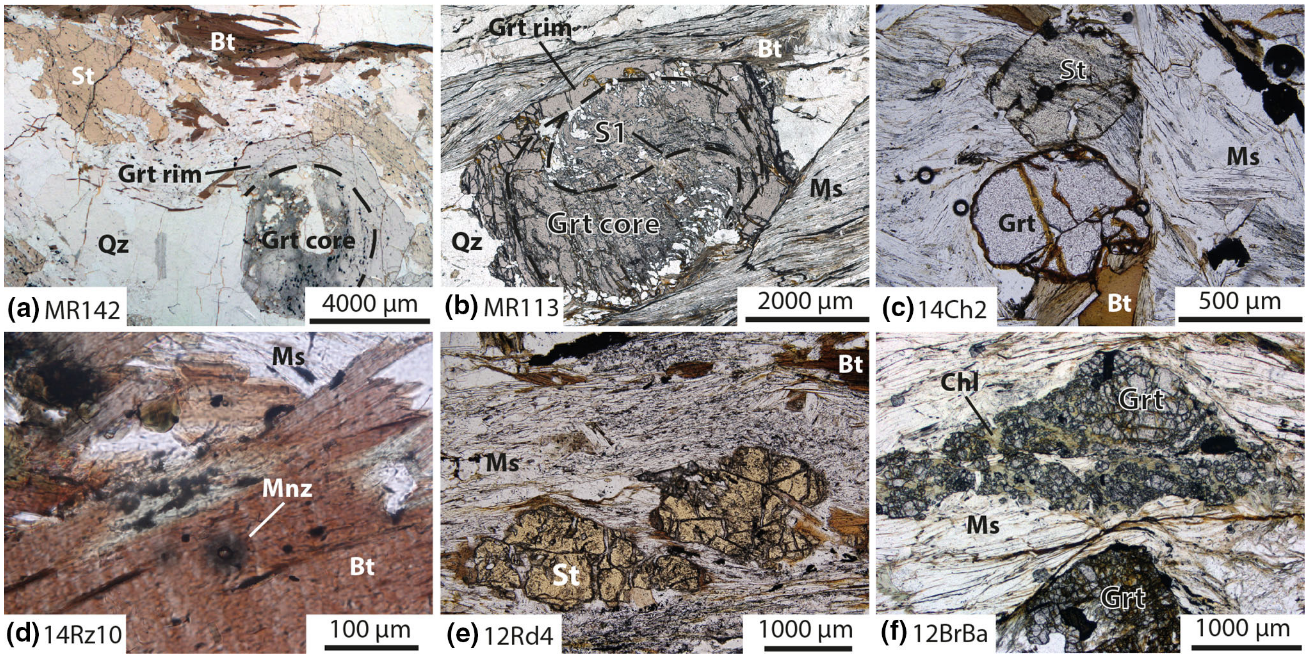

Fig. 3 Photomicrographs of thin sections illustrating the relationships between different garnet populations and chemical zoning. Sample localities are indicated in Fig. 2. Abbreviations of mineral names are after Whitney and Evans (2010). **a** Large, torn staurolite from the Baia de Arieş Unit partially engulfed by idiomorphic garnet with an inclusion-rich, embayed core; **b** large, zoned garnet with rotated inclusion trails in the core from the Bihor Unit; **c** garnet micaschist from the Ţicău inselberg exhibiting staurolite overgrowing the crenulated foliation; **d** dark haloes around monazite inclusions in biotite from the Preluca Unit (also observed in the Ţicău sample), indicating radiation damage zones; **e** large, broken staurolite grains from the Rebra Unit; **f** large, fragmented garnet porphyroclasts from the Bretila Unit

which is higher than the thermobarometric estimates from the sample (Table 2). Thus, the age should be interpreted as a formation age.

The whole rock analysis of sample MR142 shows an $\varepsilon_{Nd}(0)$ (CHUR) of -13.5, a $^{147}Sm/^{144}Nd$ ratio of $\sim$ 0.11 and yielded Sm (6.57 ppm) and Nd (35.17 ppm) contents that plot within the typical range for metapelites. Four garnet fractions were investigated and three of them show Sm and Nd concentrations in the range of 1.47–1.64 ppm and 0.26–0.31 ppm respectively. Only the second fraction grt2 was characterized by significantly higher contents of Sm (2.164 ppm) and Nd (2.641 ppm). Accordingly, the corresponding $^{147}Sm/^{144}Nd$ ratios range between 2.9 and 3.5, except for Grt2 (0.5). Unfortunately, garnet fraction grt3 was lost in the analytical process. The three remaining garnet fractions (Fig. 7a) are not concordant with the whole rock, suggesting that their deviation may be the result of the incorporation of rare element-rich inclusions that were not in equilibrium with the whole rock-garnet system. Allanite, xenotime and monazite inclusions were indeed observed in a large garnet of sample MR142 (Fig. 4c, d). However, the large scatter could also relate to mixing of different garnet populations in the sample. The data calculated for the three individual garnet fractions, together with the whole rock, cover a range of 125–176 Ma, showing a positive correlation of the $^{147}Sm/^{144}Nd$ ratio with age.

5.4 Results of monazite electron-microprobe U–Th–Pb dating

The following subchapters discuss the results of 456 individual analyses from 19 samples. Plots of the mineral chemistry and probability density plots of the monazite analyses are shown in Figs. 8 and 9. The results will be discussed individually for the Apuseni Mts., the Transylvanian Inselbergs and the Rodna Mts. in their structural order from top to bottom and from west to east. Detailed plots of the complete analytical dataset and of the individual samples are provided in Online Resources 5 and 6.

5.4.1 Apuseni Mountains

The dataset from the structurally highest Vidolm Nappe yields 25 ages forming a broad peak from Permian to Late Cretaceous ages (Fig. 9a). The results of Gaussian deconvolution show two indistinct peaks at 152 and 212 Ma. Late Jurassic to Cretaceous ages were obtained from small monazite grains, while older, Permian to Triassic ages were

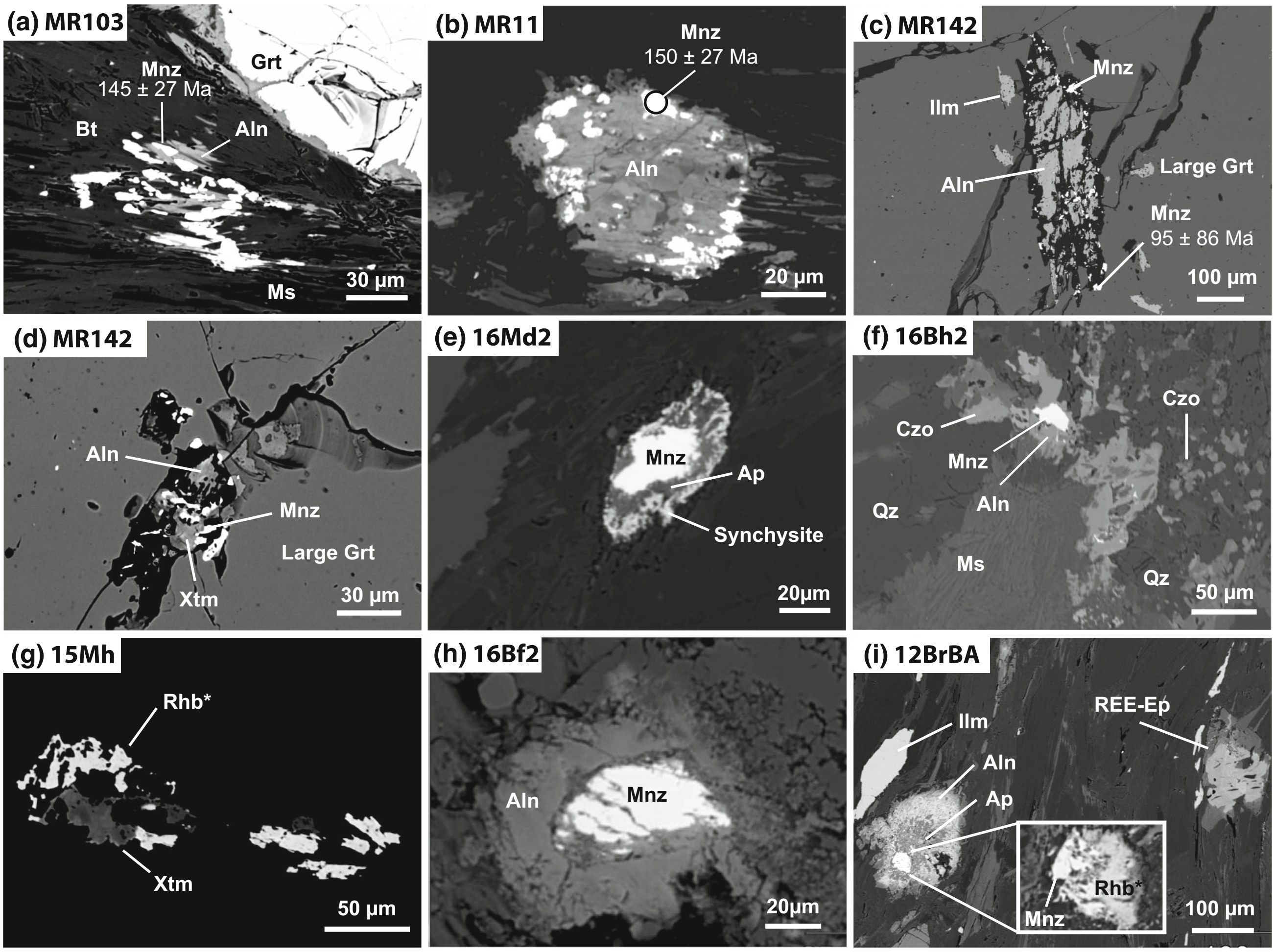

Fig. 4 Back-scattered electron (BSE) images illustrating the relationships between allanite, monazite and other REE-minerals. **a** Allanite sheaves overgrow partly resorbed monazite grains in a garnet from the Vidolm Nappe; **b** allanite from the Vidolm Nappe surrounded by "satellite" monazite grains (Finger et al. 2016); **c**, **d** in situ breakdown of allanite inclusions in garnet porphyroblasts from the Baia de Arieş Nappe. Allanite is partially (around the rims) replaced by monazite and xenotime; **e** allanite and synchysite (Y-Ce carbonates) form coronas around monazite grains in western parts of the Baia de Arieş Nappe; **f** monazite relics in the Biharia Nappe surrounded by an allanite halo with satellite monazite grains. Two samples from the Codru Unit exhibit **g** rhabdophane (Rhb*) intergrown with zoned xenotime and **h** allanite coronas around monazite grains. **i** Monazite relics in the Bretila Unit are corroded by rhabdophane (see insert), then overgrown by apatite and allanite; epidote and allanite aggregates form porphyroblasts along the foliation

obtained from large, relict grains in the matrix which often exhibit breakdown to allanite (Fig. 4a, b).

The dataset from the Baia de Arieş Nappe (Fig. 9b) exhibits a multi-modal distribution of monazite ages: two peaks of Early (411 Ma) and Late Devonian (366 Ma) ages and a sharp, more pronounced peak indicating a Late Jurassic/earliest Cretaceous age (ca. 150 Ma). Sample 16Md1 from western parts of the Baia de Arieş Nappe yields predominantly Variscan monazite ages peaking at 360 ± 14 Ma (Fig. Online Resource 6b). A few Early Palaeozoic ages were obtained from relict grains and two analyses resulted in Late Jurassic ages. The metasedimentary host-rock (sample 16Md2) yields almost exclusively Early Devonian ages (430–401 Ma; Online Resource 6c). Sample 12SJ and MR142 from the central part of the Baia de Arieş Nappe yield Late Jurassic/Early Cretaceous ages with a maximum of the probability distribution function at 149 ± 5 Ma for sample 12SJ (Online Resource 6d). Composite monazite grains from both samples show pre-Alpine cores and Th-rich (19.29 wt%) Alpine overgrowth (e.g. Fig. 5c), but Alpine growth zoning can be observed as well (sample 12SJ; Fig. 5e). The low number (n = 6) of analyses from the Biharia Unit (sample 16Bh2) does not allow for a meaningful interpretation and will not be used for further discussion.

The dataset of the Codru Unit (Fig. 9c) is hampered by very small monazite grains and abundant rhabdophane minerals that are difficult to date. However, the results of 19 analyses from samples 16Bf2 (from the Codru Mts. in the western part of the study area) and 15Mh (a tectonic

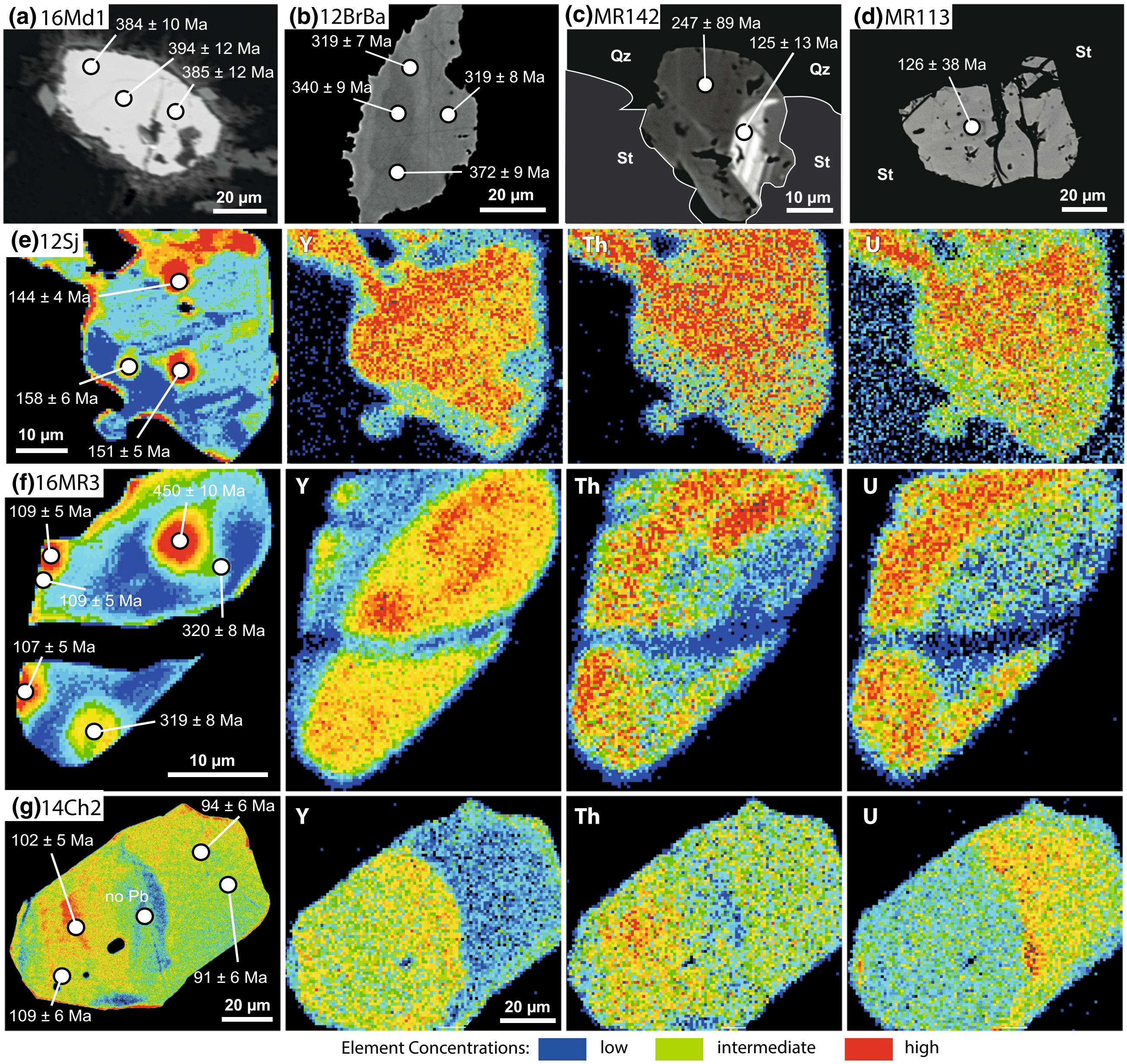

Fig. 5 Back-scattered electron (BSE) images. Ages and location of U-Th–Pb analyses are indicated. **a** Pre-Alpine monazite in sample 16Md1 exhibits an allanite corona and euhedral zircon growth, **b** compositional zoning in a pre-Alpine monazite from sample 12BrBA; **c** distinctly zoned composite monazite overgrowing a staurolite grain. The grain boundary of the staurolite was graphically enhanced to illustrate the correlation between the internal zoning in the monazite and the overgrown area; **d** a subhedral to rounded grain forming an inclusion in staurolite from the Bihor Unit; **e** BSE image and compositional map (Y, Th, U) from a monazite inclusion in a garnet porphyroblast from the Baia de Arieş Nappe); **f** BSE image and compositional map of a composite monazite from the Bihor Unit showing strong zonation of Th, Y and U correlating with different age clusters; **g** BSE image and element distribution maps of dated monazite from sample 14Ch2 (Ţicău Inselberg). Element distribution maps were produced using XMap from Bernhardt et al. (1995)

window beneath the Biharia Nappe) show a dominant Early Carboniferous peak (337 Ma; Fig. 9c) that correlates with elevated Y contents in the analyses (Fig. 8b).

The analysed samples from the Bihor Unit in the Apuseni Mts. show a multi-modal distribution of ages which consists of a broad Carboniferous to Early Triassic cluster (∼ 350–240 Ma) split into several sub-peaks and a sharp Early Cretaceous peak (106 Ma; Fig. 9d). Alpine ages were obtained from euhedral, inclusion-rich monazite grains from structurally higher parts of the Bihor Unit (Fig. 5d and f; samples MR113 and 16MR3, Online Resource 6i, j). Sample 16MR3 also exhibits a remarkable

Table 2 Results of *P*–*T* calculations using Thermocalc (Grt-Bt thermometry) and results of Ti-in-biotite calculations ("n" refers to the number of analyses from which the weighted average was calculated)

Tectonic unit	Sample#	Average PT								Ti in biotite		
		P [GPa]	SD	T [°C]	SD	Corr	Sig fit	Sig max	NIR	n	T [°C]	2σ
Bihor unit	MR32	0.8	± 0.1	544	± 87	0.833	0.35	1.96	3	–	–	–
	MR113	0.8	± 0.1	532	± 82	0.764	0.21	1.73	4	6	548	± 19
Baia de Arieş Nappe	MR61	0.5	± 0.2	536	± 18	0.394	1.38	1.73	4	–	–	–
	MR15	0.7	± 0.1	545	± 87	0.817	0.17	1.73	4	8	566	± 17
	MR142	–	–	495	± 79	0.788	0.62	1.96	3	6	556	± 39
Vidolm Nappe	MR11	1.1	± 0.1	635	± 80	0.925	0.88	1.73	4	9	584	± 31
	MR103	0.8	± 0.1	501	± 77	0.844	0.92	1.96	3	–	–	–

For detailed chemical data, see Online Resource 3

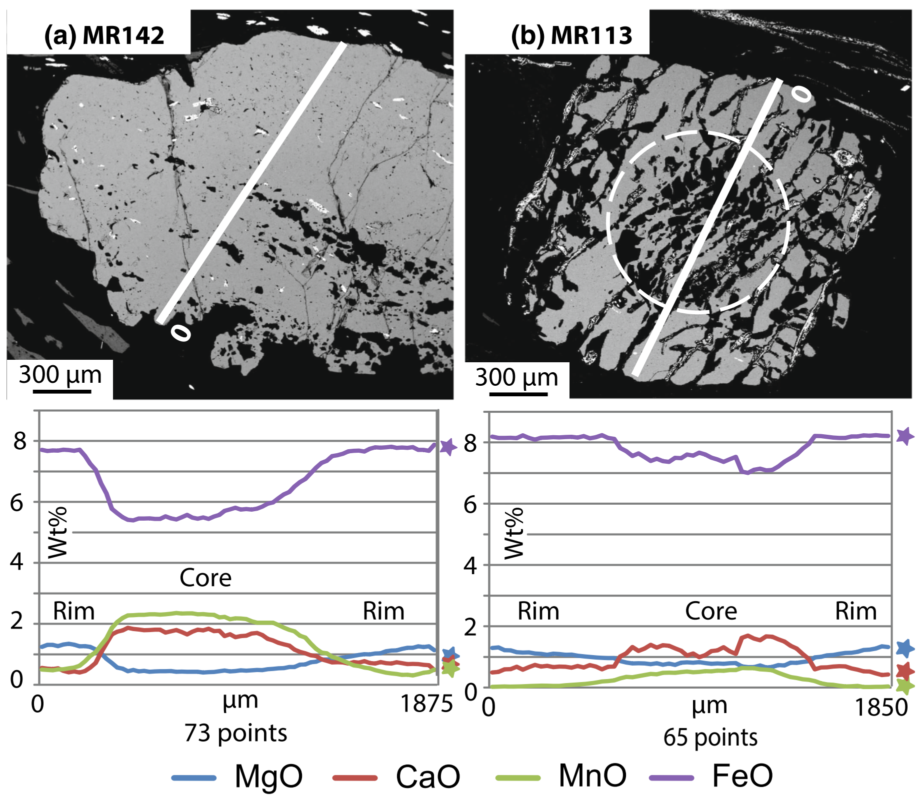

Fig. 6 Back-scattered electron (BSE) images of representative garnet from samples **a** MR142 and **b** MR113 together with their chemical profiles based on electron microprobe analyses (see also Online Resources 3 and 4). Star symbols to the right of the profiles represent analyses of a smaller, un-zoned garnet population present in both samples. The zoning profile for sample MR142 is typical for garnet (almandine) formed under low-amphibolite-facies *P*–*T* conditions and shows a prograde Mn-bell profile due to the substitution of Fe for Mn. Sample MR113 exhibits an even less developed zoning pattern, the dashed circle marks the rotated core of sample MR113

bi-modal age distribution (Fig. 8d) with a strong Carboniferous to Permian age range and a subpeak of Triassic ages. Internal parts of the Bihor Unit (sample 14Hm) yield exclusively Variscan age distributions (366–306 Ma; Online Resource 6k).

5.4.2 Transylvanian Inselbergs

The samples from the Şimleu Silvaniei, Ţicău and Preluca inselbergs are shown as individual plots (Fig. 9e–g). Sample 16Sm1 from the Şimleu Silvaniei Inselberg yields a broad Permo-Triassic age peak (∼ 300–230 Ma) and several smaller subpeaks (Fig. 9e). Meanwhile, the samples from the Ţicău and Preluca inselbergs (Fig. 9f and g) show good agreement in their exclusively Alpine ages (around 100 Ma). The age distribution in sample 14Ch2 from the Ţicău inselberg (101 Ma; Fig. 9f) is coherent with the ages obtained from core/rim of individual crystals (Fig. 5 g) and overlaps with the almost perfect Gaussian age distribution from the Preluca sample (14Rz10;

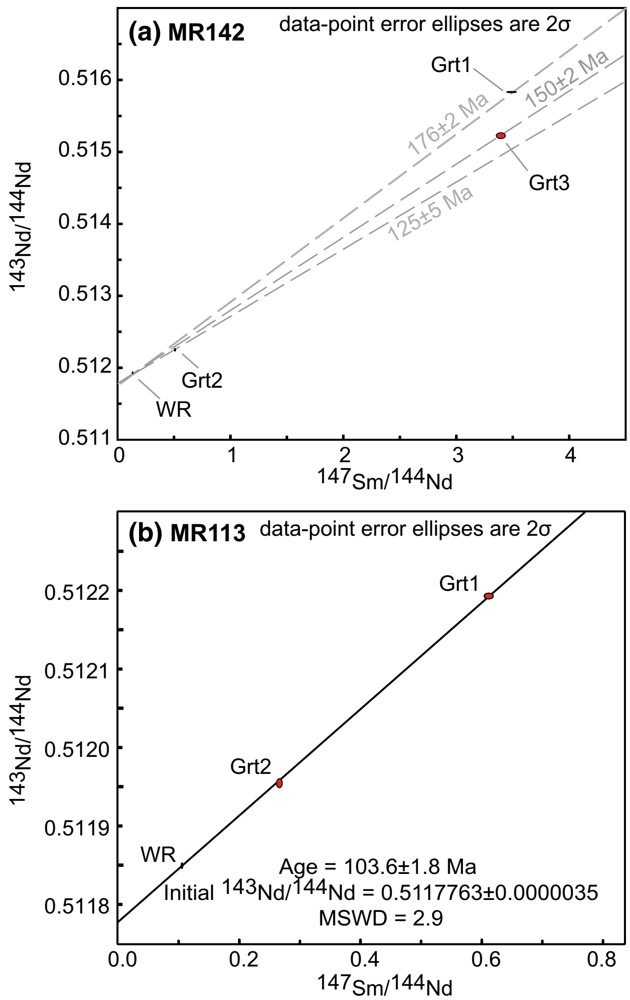

Fig. 7 Sm-Nd whole rock-garnet analyses from **a** the Baia de Arieş Nappe and **b** the Bihor Unit. No isochron was calculated for sample MR142, but dates of individual garnet fractions are shown as dashed lines

Fig. 9 g). Monazite from the latter is characterized by low yttrium content (Fig. 8b).

5.4.3 Rodna Mountains

The dataset from the Rodna Mts. (Fig. 9 h) yields two different age clusters: sample 12Rd4 from the Rebra Unit shows exclusively mid- to Late Cretaceous ages (105–80 Ma) while the—probably not fully representative—dataset of sample 12BrBA (n = 13) yields only pre-Alpine ages from zoned monazite (Fig. 5b), that cluster around 318 Ma.

6 Discussion

6.1 Data from the Apuseni mountains

6.1.1 Vidolm Nappe (Dacia Mega-Unit)

Pre-Alpine ages from relict grains in samples MR11 and MR103 (Fig. 9a) show good agreement with Jurassic and Permo-Triassic age clusters in detrital zircon populations (170–200 Ma and 250–300 Ma) reported from Late Cretaceous Gosau-type sediments in the vicinity (Schuller et al. 2009). The observed monazite breakdown reactions (Fig. 4a, b) are interpreted as the consequence of a less pervasive Alpine overprint at thermal conditions between 400 and 450 °C (Finger et al. 1998). Together with other thermochronological data (Kounov and Schmid 2013; Reiser et al. 2017), the Cretaceous thermal overprint is constrained to not exceed greenschist facies conditions. It follows, that the thermobaric estimates reported in Table 2 relate to a pre-Alpine overprint.

6.1.2 Baia de Arieş Nappe (Dacia Mega-Unit)

Late Silurian/Early Devonian ages (430–400 Ma; sample 16Md2) from metasedimentary rocks in western parts of the Baia de Arieş Nappe are difficult to constrain. Nevertheless, they can be interpreted to reflect a pre-Variscan thermo-tectonic or magmatic event. Variscan ages from sample 16Md1 (360 ± 14 Ma) correlate perfectly with the emplacement age of the Mădrigeşti granite (364 ± 2 Ma; Pană et al. 2002). In both samples (16Md1 and 16Md2), a weak, post-Variscan overprint is recorded by the formation of coronas or clusters of allanite around monazite (Figs. 4e and 5a) indicating prograde destruction of the latter under thermal conditions below the biotite-in isograd (cf. Finger et al. 1998). An outlier of two Middle to Late Jurassic ages allows inferring a tentative age for this overprint (cf. Online Resource 6b). In the eastern part of the Baia de Arieş Nappe, the results from samples 12SJ and MR142 show a correlation between high Th/U ratios and Late Jurassic–Cretaceous ages (Fig. 8a). According to Pyle et al. (2005), Th-rich cores relate to strong Rayleigh-type fractionation of Th during early stages of monazite growth where Th is available from the surrounding. Possible sources of Th for monazite growth are grain boundaries (cf. Corrie and Kohn 2008), tiny $ThSiO_4$ grains, breakdown of allanite minerals or overgrown staurolite grains, all of which can be observed in samples 12Sj and MR142 (Fig. 4c, d). Late Jurassic/Early Cretaceous monazite grains overgrowing staurolite (Fig. 5c), as well as monazite inclusions in garnet and staurolite indicate their formation on the prograde path,

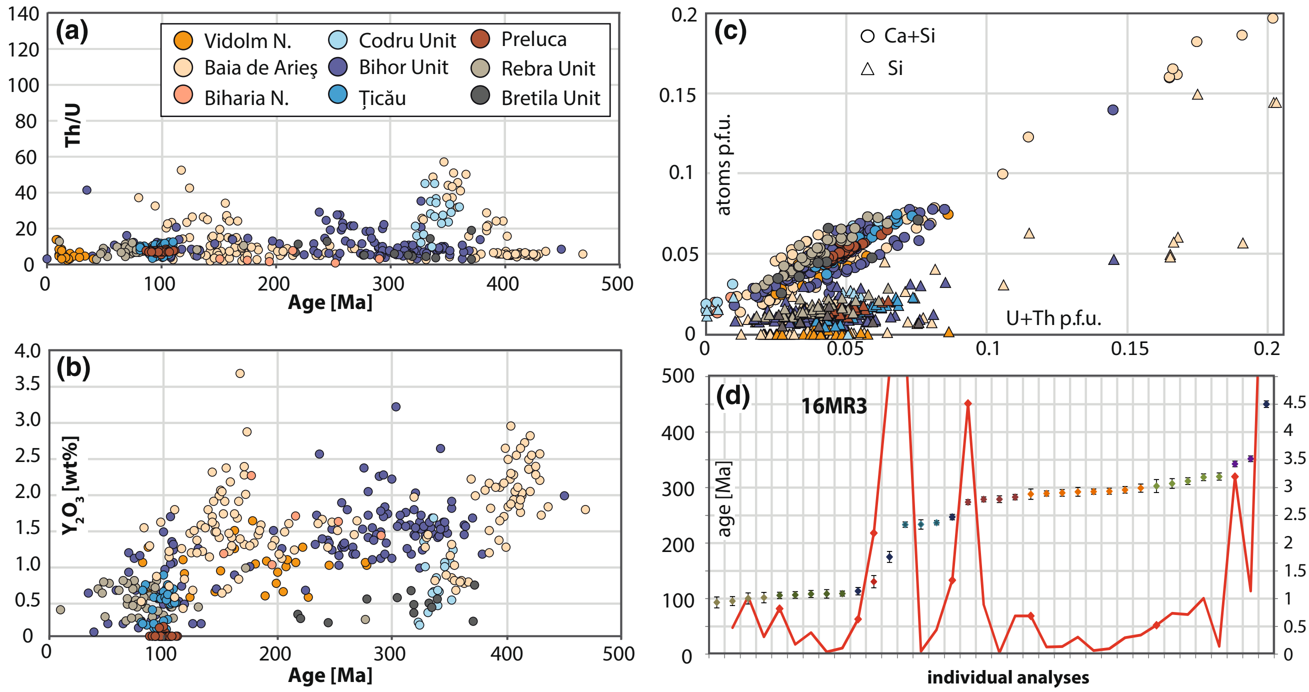

Fig. 8 Mineral chemistry and distributions of monazite Th-U–Pb chemical ages: **a** age vs. Th/U; **b** age vs. Y_2O_3; **c** Si + Ca and Si (apfu) vs. U + Th (apfu) diagram; **d** age distribution plot with error-normalized age gradients used to separate domain boundaries (thick red line)

i.e. prior to, or simultaneous with crystallization of these porphyroblasts. Allanite breakdown reactions are observed in garnet and call for thermal (peak) conditions of ~ 525–600 °C (Kohn and Malloy 2004; Spear 2010; Spear and Pyle 2010), which shows good agreement with the thermobaric estimates presented in Table 2. Small grain sizes of monazite neoblasts surrounding these allanite inclusions (≤ 5–10 µm; Fig. 4c, d) and very low Pb contents, at or below the detection limit (≤ 100 ppm) prevent the acquisition of reliable age data. However, these LREE inclusions in the garnet are likely responsible for the observed differences in the results of individual garnet batches of sample MR142 (see discussion in Sect. 5.3). The range of Sm–Nd garnet dates from sample MR142 between 176 and 125 Ma (Fig. 7a) coincides with the broad peak of Alpine ages from monazite analyses (ca. 150 Ma; Fig. 9b). Yttrium-poor rims of zoned monazite grains (Fig. 5e) presumably relate to fractionation during garnet-growth at peak conditions. Ar–Ar hornblende ages (118/119 Ma; Dallmeyer et al. 1999) indicate cooling below the 500 °C isotherm and thus represent a minimum age for garnet growth in the Baia de Arieş Nappe. Together with T-t paths from previous studies (Reiser et al. 2017), we correlate the Early Cretaceous peak of monazite ages in the Baia de Arieş Nappe (Fig. 9b) with the prograde formation of a medium-grade assemblage (Fig. 3a).

6.1.3 Bihor and Codru units (Tisza Mega-Unit)

Although the dataset from the Codru Unit (samples 16Bf1, 16Bf2, 15Mh) is hampered by intense domination of rhabdophane in the samples, it yields a clear Variscan peak of monazite ages (337 Ma; Fig. 9c) that closely correlates with Variscan Ar–Ar ages from Dallmeyer et al. (1999). Petrographic observations show a weak Alpine overprint (cf. thick allanite corona surrounding the monazite in Fig. 4 g), which is constrained to less than ~ 300 °C by pre-Alpine zircon fission track ages from the vicinity of sample 16Bf2 (Reiser 2015). Ages that cluster around 180 Ma possibly represent mixed ages between Variscan and Alpine overprints. Altogether, we conclude that the Codru Unit experienced medium-grade conditions during a Variscan event that was overprinted under low-grade conditions during the Alpine evolution. In the vicinity of the nappe contact with the overlying Codru Unit, the obtained Sm–Nd garnet age from sample MR113 (103.6 ± 1.8 Ma; Fig. 7b) shows good agreement with the ages from Y-poor rims of zoned monazite from sample 16MR3 (Fig. 5f). This correlation can be explained by strong fractionation of Y during garnet growth (e.g. Spear and Pyle 2010; Schulz 2016). Permo-Triassic ages from the same sample (285–242 Ma; Fig. 8d) presumably relate to the emplacement of the Muntele Mare pluton (291 ± 3 Ma; Balintoni et al. 2009a) and/or the

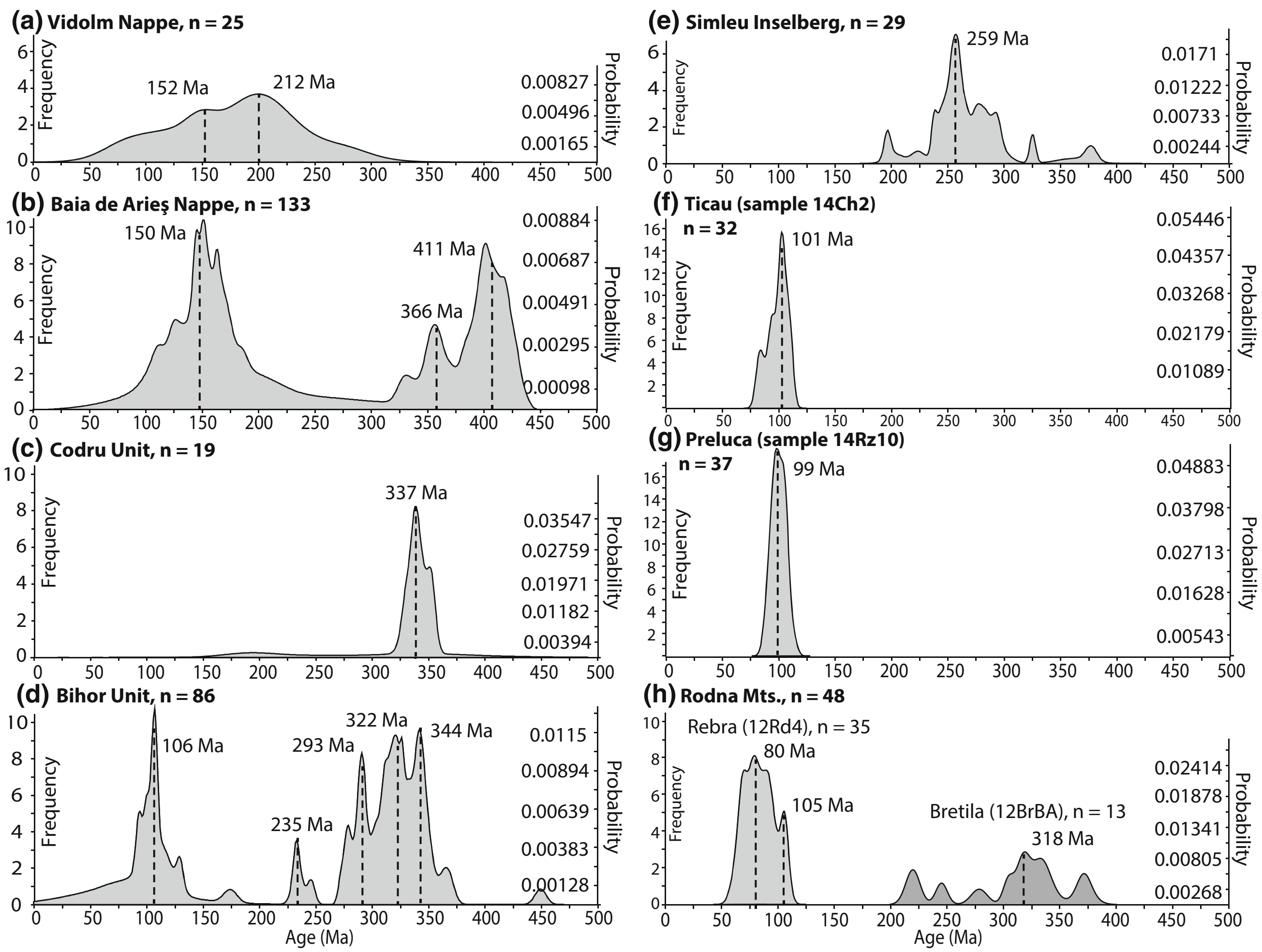

Fig. 9 Stacked chart of probability density plots of monazite ages. **a** Vidolm Nappe (samples MR11 and MR103); **b** Baia de Arieş Nappe (samples MR142, 12Sj, 16Md1, 16Md2); **c** Codru unit (samples 16Bf2, 15Mh); **d** Bihor Unit (samples MR113, 16MR2, 16MR3, 14Hm); **e** Şimleu Silvaniei Inselberg (sample 16Sm1); **f** Ţicău (sample 14Ch2); **g** Preluca (sample 14Rz10); **h** Rodna Mts. (composed of samples 12Rd4 and 12BrBA). Plots were produced with a fixed bin size (10 Ma) using the program jagedisplay v1.0 (Thomsen et al. 2016). Peaks in the probability density of ages for plots **a**, **b**, **d**, **e** and **h** are obtained through un-mixing multicomponent data using Gaussian deconvolution in Isoplot v4.15 (Ludwig 2012); the remaining peaks are calculated maxima of the probability density function

emplacement of pegmatites in central parts of the Bihor Unit (242 ± 16 Ma Rb–Sr WR; Anton 1999). Variscan ages from sample 16MR3, correlate with the Variscan peak from internal parts of the Bihor Unit (sample 14Hm; Online Resource 6 k). This is in good agreement with other geochronological data from the same area (Soroiu et al. 1985; Pavelescu et al. 1975; Dallmeyer et al. 1999). We conclude that the Bihor Unit was affected by Permo-Triassic magmatic events and experienced polyphase medium-grade overprinting during Variscan and Alpine events.

6.2 Data from the Transylvanian Inselbergs

Permo-Triassic ages from the Şimleu Silvaniei Inselberg (sample 16Sm1) indicate a distinct phase of monazite formation presumably related to magmatic processes that also affect the neighbouring Bihor Unit (see discussion in the previous section). Monazite inclusions observed in sample 14Ch2 from the Ţicău Inselberg, considered as a part of Tisza, indicate their crystallization prior to or contemporaneously with biotite and garnet formation. Zoned monazite grains show late Early Cretaceous ages in the core and early Late Cretaceous ages in the low-Y rim (Fig. 5g). Denuţ (1998) and Radu (2003) reported polyphase garnet growth during two prograde events. Accordingly, the monazite crystallized during a late Early Cretaceous medium-grade metamorphic event, that overprinted a pre-existing medium-grade assemblage and fabric (Fig. 3c). Monazite ages from the Preluca Inselberg, considered as a part of Dacia, show a mid-Cretaceous peak very similar to that of the Ţicău dataset (Fig. 8c, d). The absence of allanite in sample 14Rz10 and the fact that monazite grains are mainly preserved as inclusions in large biotite flakes (Fig. 3d) and garnet, indicates the crystallization of metamorphic monazite together with a medium-grade assemblage. The observed low-Y contents of the analyses from Ţicău and Preluca (Fig. 8b) thus indicate fractionation of Y associated with garnet-growth (Spear and Pyle 2010; Schulz 2016) during a medium-grade overprint, rather than a low-temperature formation (cf. Krenn and Finger 2007). K–Ar hornblende, biotite and muscovite cooling ages from the Preluca Inselberg (Soroiu et al. 1985; Zincenco et al. 1990) strengthen the argument for a metamorphic overprint affecting the Ţicău and Preluca inselbergs during late Early Cretaceous times.

6.3 Data from the Rodna Mountains

The dataset from the Rebra Unit yields a peak of ages at around 80 Ma (Fig. 9 h). Although the dataset from the Bretila Unit is limited by the low abundance of suitable monazite, the Variscan age peak with Devonian and Permo-Triassic clusters is significantly different from the data from the Rebra Unit, which lack Variscan ages. According to Kräutner et al. (1976), this probably relates to a differential Alpine overprint, localized in the southwest of the Rodna Mts. Allanite overgrowth on monazite in the Bretila Unit (sample 12BrBa; Fig. 4i) evidences a second metamorphic event at thermal conditions around the chloritoid-biotite isograd, where allanite crystallizes at the expense of detrital monazite ($\sim$ 400–450 °C, $\sim$ 0.4 GPa; Wing et al. 2003; Janots et al. 2007, 2008; Spear 2010). The presence of two-garnet generations, rutile-ilmenite-titanite overgrowth as well as Alpine and pre-Alpine K–Ar ages (Kräutner et al. 1976) indicate a polymetamorphic evolution of the Rodna Mountains. Permo-Triassic and mid-Cretaceous Ar–Ar single grain ages from mylonitic schists of the Bretila Unit (Culshaw et al. 2012) strengthen the argument for an Alpine overprint. Strutinski et al. (2006) postulated a lower amphibolite facies event during Early Cretaceous times, followed by fast cooling during the Albian to early Late Cretaceous.

6.4 Metamorphic evolution

6.4.1 Pre-Alpine monazite ages (Ordovician to Carboniferous)

Monazite ages older than 300 Ma are often preserved in the core of zoned monazite, or as relict grains surrounded by allanite coronas. Several ages older than 400 Ma, obtained from the Codru and Bihor Units (Fig. 5f), presumably relate to Ordovician magmatic activity (i.e. 470–450 Ma; Pană et al. 2002; Balintoni et al. 2009a, b). An age cluster around 411 Ma from sample 16Md2; Baia de Arieş Nappe) could either indicate a later magmatic or thermal event (e.g. Caledonian metamorphism; Zincenco et al. 1990). Ages between 300 and 370 Ma (encountered in the Baia de Arieş Nappe, Codru Unit, Bihor Unit and Bretila Unit) are attributed to the generation of a medium-grade mineral assemblage during the Variscan orogeny. This mineral assemblage comprises almandine ± staurolite ± kyanite in a primary foliation (s1) which can be observed in several basement exposures of the Apuseni Mountains (Baia de Arieş Nappe and Bihor Unit; Mârza 1969; Balintoni and Iancu 1986; Hârtopanu and Hârtopanu 1986; Dimitrescu 1994), the Transylvanian inselbergs (Kalmár 1996; Kalmár and Kovács-Pálffy 1996; Radu 2003) and the Rodna Mts. (Mosonyi 1999; Culshaw et al. 2012). Late Variscan Ar–Ar hornblende and muscovite ages, reported from the northern part of the Apuseni Mts. (Dallmeyer et al. 1999), from metamorphic rocks of the Algyő High (Lelkes-Felvári et al. 2003) and the Eastern Carpathians (Strutinski et al. 2006) correlate with the Variscan overprint.

6.4.2 Occurrences and significance of Permo-Triassic ages

Monazite ages ranging between 200 and 300 Ma are predominantly observed in the Bihor Unit and in several relict grains from the Vidolm Nappe. These ages coincide with the age of emplacement of several magmatic intrusions in the Apuseni Mts. (e.g. the Muntele Mare pluton and the Highiş-Biharia igneous complex; Pana et al. 2002; Balintoni et al. 2009a) and the emplacement of pegmatites in the central part of the Bihor Unit (245 Ma; Anton 1999). A "late-Variscan" low-pressure, high-temperature regime (550-600 °C, 2–3 kbar, sillimanite/andalusite zone) is reported from the basement of the Tisza Mega-Unit in Hungary (Lelkes-Felvári et al. 1989, 2005; Szederkényi et al. 2012; Haas and Budai 2014). Sillimanite overgrowth on kyanite, which presumably correlates with this low-P/high-T event, is reported from the central part of the Bihor Unit (Hârtopanu and Hârtopanu 1986) and the Preluca Inselberg (Radu 1997). Furthermore, Permo-Triassic ages from our study show good agreement with geochronological data from several surrounding areas such as the Algyő High (273 Ma Sm–Nd garnet age; Lelkes-Felvári et al. 2003), the Slavonian Mts. (Balen et al. 2013, 2017), the Rodna Mts. (Culshaw et al. 2012), the Serbo-Macedonian massif (Antić et al. 2017), and the Eastern Alps (Schuster and Stüwe 2008; Schuster et al. 2015; Thöni et al. 2008; Thöni and Miller 2009).

6.4.3 Early Cretaceous medium-grade overprint

Newly formed monazite grains and overgrowths of Early Cretaceous age indicate a metamorphic overprint in the Baia de Arieş Nappe (Dacia Mega-Unit) that resulted in the formation of a secondary, medium-grade mineral assemblage. Results from *P*–*T* analyses, together with petrographic observations confirm medium-grade thermal conditions that are also reported for the allanite to monazite transition in typical metapelites (525–600 °C; Janots et al. 2007; Spear 2010). The timing of this overprint correlates with top-NE directed nappe stacking reported for the Biharia Nappe System of the Dacia Mega-Unit (D1 sensu Reiser et al. 2017a). The late Early Cretaceous Sm–Nd garnet age (103.6 ± 2 Ma; sample MR113; Fig. 7) from the Bihor Unit evidences Alpine garnet growth in the Tisza Mega-Unit. Comparable U–Th–Pb monazite ages from the Bihor Unit, the Preluca and Ţicău inselbergs, as well as the Rebra Unit in the Rodna Mts. provide further evidence for a medium-grade overprint at the contact between the Tisza and Dacia mega-units during late Early Cretaceous times. This presumably correlates with late Early Cretaceous top-NW directed thrusting in the Apuseni Mountains (D2; Reiser et al. 2017a). A basement sliver of the Codru Unit (largely unaffected by Alpine metamorphism; Dallmeyer et al. 1999; Reiser et al. 2017a) at the contact between the Bihor Unit (Tisza Mega-Unit) and the Biharia Nappe System (Dacia Mega-Unit) separates the metamorphic overprints: Early Cretaceous metamorphism (D1) affects the Dacia Mega-Unit following the obduction of the Transylvanian Ophiolites, while late Early Cretaceous metamorphism (D2) overprints the contact between the Tisza and Dacia mega-units. The thermal contrast between the Bihor and Codru units is a consequence of Late Cretaceous exhumation along low-angle detachments (Reiser et al. 2017a).

On a regional scale, the distribution of Cretaceous medium- to high-grade metamorphism in the ALCAPA, Tisza and Dacia mega-units defines two belts (Fig. 10). When these mega-units are back-rotated to their pre-Miocene arrangement (using palaeomagnetic data and palaeogeographic reconstructions, e.g. Pătraşcu et al. 1994; Márton 2000; Márton and Fodor 2003; Márton et al. 2007; Ustaszewski et al. 2008; Lorinczi and Houseman 2010), the Cretaceous metamorphic overprint forms a continuous belt

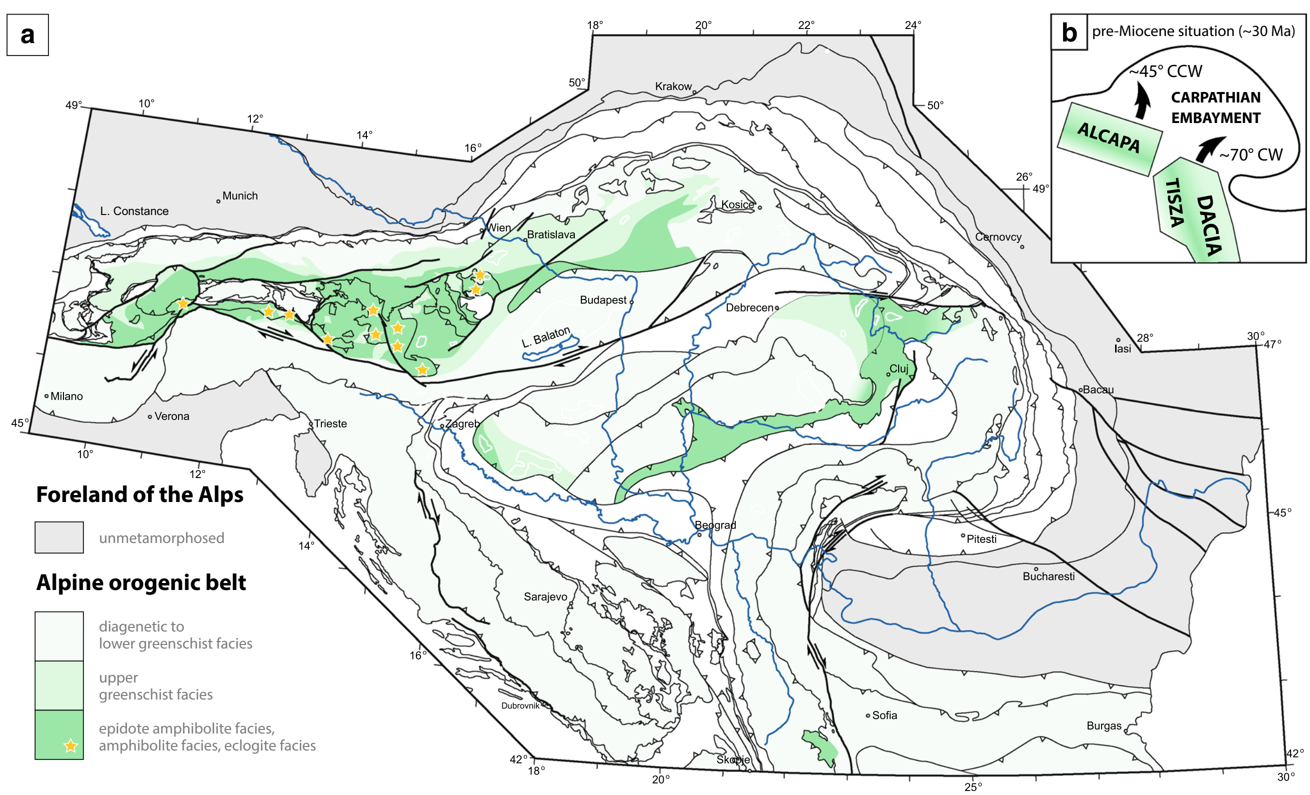

Fig. 10 **a** Map illustrating the distribution of Cretaceous metamorphism in the ALCAPA, Tisza and Dacia mega-units (modified from Schmid et al. 2008; compare Fig. 1). Information on the timing and degree of metamorphism is based on Antić et al. (2016); Árkai et al. (2000); Balen et al. (2013, 2017); Ciulavu et al. (2008); Culshaw et al. (2012); Dallmeyer et al. (1996, 1999); Froitzheim et al. (2008); Gröger et al. (2013); Hoinkes et al. (1999); Iancu et al. (2005); Janák et al. (2004, 2015); Jeřábek et al. (2012); Kalmár (1996); Koroknai et al. (2001); Kounov et al. (2010); Lelkes-Felvári et al. (1996); Lelkes-Felvári et al. (2003); Schuster et al. (2004); Soroiu et al. (1985); Strutinski et al. (2006); van Gelder et al. (2015); Vojtko et al. (2016, 2017); Zincenco et al. (1990) and the results from this study. **b** Sketch of the situation along the European continental margin during pre-Miocene times. Rotational movements are indicated based on palaeomagnetic data and palaeogeographic reconstructions (Pătraşcu et al. 1994; Márton 2000; Márton and Fodor 2003; Márton et al. 2007; Ustaszewski et al. 2008; Lorinczi and Houseman 2010)

(schematically shown on Fig. 10b). This presumably reflects the palaeogeographic position and arrangement of these mega-units along the southern continental margin of the European plate during the Cretaceous. Furthermore, this offers new constraints for correlating tectonic events in the Alps-Carpathians-Dinarides orogenic system.

7 Conclusions

The presented dataset further constrains location and timing of medium-grade metamorphism in the Tisza and Dacia mega-units. Medium-grade mineral assemblages in the basement units of the study area are dated as being related to (pre-)Variscan, Permian and Alpine metamorphic events. Early to late Early Cretaceous crystallization of metamorphic monazite grains at or close to peak metamorphic conditions concurs with Sm–Nd garnet analyses in the respective tectonic units. Accordingly, the data presented document a medium-grade metamorphic overprint in the Dacia Mega-Unit during the Early Cretaceous. Additionally, a distinct overprint during late Early Cretaceous times is indicated for the contact area between the Tisza and Dacia mega-units. Although scattered and often obscured, there is widespread evidence for prograde Alpine metamorphism in parts of both Tisza and Dacia mega-units. This metamorphism possibly correlates with the Cretaceous (Eo-Alpine) overprint of the ALCAPA Mega-Unit in the Eastern Alps. The results of this study call for further investigations on the distribution and zoning of the post-Variscan overprint across the Transylvanian and Pannonian basins, providing important additional constraints on the palaeogeographical arrangement of the ALCAPA, Tisza and Dacia mega-units in Cretaceous times.

Acknowledgements We thank Martina Tribus and Thomas Theye for helping with the microprobe analyses, Stanislaw Grabala and Andrea Eberhöfer for help with the mineral separation and Monika Horschinegg and Wencke Wegner for chemical preparation and isotope measurements. Financial support by the Austrian Science Fund (FWF) in the frame of project I138-N19, granted to Bernhard Fügenschuh and the Romanian Executive Unit for Financing Research and Higher Education (UEFISCDI), project PN-II-ID-PCE-2011-3-0030, granted to Gavril Săbău are gratefully acknowledged. We would like to thank Vladica Cvetković, S.M. Schmid, F. Finger and an anonymous reviewer for careful reading and constructive comments that significantly improved the manuscript.

References

Antić, M. D., Kounov, A., Trivić, B., Spikings, R., & Wetzel, A. (2017). Evidence of Variscan and Alpine tectonics in the structural and thermochronological record of the central Serbo-Macedonian Massif (south-eastern Serbia). *International Journal of Earth Sciences, 106*(5), 1665–1692.

Antić, M. D., Kounov, A., Trivić, B., Wetzel, A., Peytcheva, I., & von Quadt, A. (2016). Alpine thermal events in the central Serbo-Macedonian Massif (southeastern Serbia). *International Journal of Earth Sciences, 105*(5), 1485–1505.

Anton, D.C. (1999). Petrographical, Geochemical and Isotopic Study of Mt. Mare Granitoids, North Apuseni Mountains: Evolution of Peraluminous Magma. *Ph.D. dissertation*, Tokyo University, Japan, pp. 176.

Árkai, P. (2001). Alpine regional metamorphism in the main tectonic units of Hungary: A review. *Acta Geologica Hungarica, 44*(2–3), 329–344.

Árkai, P., Bérczi-Makk, A., & Balogh, K. (2000). Alpine low-T prograde metamorphism in the post-Variscan basement of the Great Plain, Tisza Unit (Pannonian Basin, Hungary). *Acta Geologica Hungarica, 43*(1), 43–63.

Árkai, P., Bérczi-Makk, A., & Hajdu, D. (1998). Alpine prograde and retrograde metamorphisms in an overthrusted part of the basement, Great Plain, Pannonian Basin, Eastern Hungary. *Acta Geologica Hungarica, 41*(2), 179–210.

Balen, D., Horváth, P., Finger, F., & Starijaš, B. (2013). Phase equilibrium, geothermobarometric and xenotime age dating constraints on the Alpine metamorphism recorded in chloritoid schists from the southern part of the Tisia Mega-Unit (Slavonian Mts., NE Croatia). *International Journal of Earth Sciences, 102*(4), 1091–1109.

Balen, D., Massonne, H. J., & Lihter, I. (2017). Alpine metamorphism of low-grade schists from the Slavonian Mountains (Croatia): new PT and geochronological constraints. *International Geology Review, 60*(3), 288–304.

Balintoni, I. (1982). Corrélation des unités lithostratigraphiques et tectoniques longeant le ruisseau d'Arieş entre la vallée de Iara et le Mont Găina (Monts Apuseni). *Dări de Seamă ale Şedinţelor—Institutul de Geologie şi Geofizică, 69*(5), 5–15.

Balintoni, I. (1994). Structure of the Apuseni Mts. ALCAPA II. Field Trip Guidebook. *Romanian Journal of Tectonics and Regional Geology, 75*(2), 51–58.

Balintoni, I., Balica, C., Cliveti, M., Li, L. Q., Hann, H. P., Chen, F. K., et al. (2009a). The emplacement age of the Muntele Mare Variscan granite (Apuseni Mountains, Romania). *Geologica Carpathica, 60*(6), 495–504.

Balintoni, I., Balica, C., Ducea, M. N., Chen, F. K., Hann, H. P., & Sabliovschi, V. (2009b). Late Cambrian-Early Ordovician Gondwanan terranes in the Romanian Carpathians: A zircon U-Pb provenance study. *Gondwana Research, 16*(1), 119–133.

Balintoni, I., Balica, C., Ducea, M. N., & Hann, H. P. (2014). Peri-Gondwanan terranes in the Romanian Carpathians: A review of their spatial distribution, origin, provenance, and evolution. *Geoscience Frontiers, 5*(3), 395–411.

Balintoni, I., Balica, C., Ducea, M. N., Zaharia, L., Chen, F. K., Cliveti, M., et al. (2010). Late Cambrian-Ordovician northeastern Gondwanan terranes in the basement of the Apuseni Mountains, Romania. *Journal of the Geological Society, 167*(6), 1131–1145.

Balintoni, I., & Gheuca, I. (1977). Progressive metamorphism, retrogressive metamorphism, and tectonics in Zugreni-Barnar region (Eastern Carpathians). *Dări de Seamă ale Şedinţelor-Institutul de Geologie si Geofizică, 63*, 11–38.

Balintoni, I., Gheuca, I., & Voda, A. (1983). Alpine and Hercynian overthrust nappes from central and southern areas of the east Carpathians Crystallin-Mesozoic Zone. *Anuarul Institutului Geologic al României, 60*, 15–22.

Balintoni, I., & Iancu, V. (1986). Lithostratigraphic and tectonic units in the Trascău Mountains, north of Mănăstirea Valley. *Dări de*

Seamă ale Şedinţelor—Institutul de Geologie şi Geofizică, 70–71(5), 45–56.

Balintoni, I., Mosonyi, E., & Puste, A. (1997). Informaţii si interpretari litostratigrafice, metamorfice si structurale privitoare la masivul Rodna (Carpaţii Orientali). *Studia Universitatis Babeş-Bolyai, Geologia, 42*(2), 51–66.

Balintoni, I., Puşte, A., & Stan, R. (1996). The Codru nappe system and the Biharia nappe system: A comparative argumentation. *Studia Universitatis Babeş-Bolyai, Geologia, 41*(1), 101–113.

Balla, Z. (1987). Tertiary palaeomagnetic data for the Carpatho-Pannonian region in the light of Miocene rotation kinematics. *Tectonophysics, 139*(12), 67–98.

Bernhardt, H., Massonne, H., Reinecke, T., Reinhardt, J., & Willner, A. (1995). Digital element distribution maps, an aid for petrological investigations. *Berichte der Deutschen Mineralogischen Gesellschaft, Beihefte zum European Journal of Mineralogy, 7*(1), 28.

Bleahu, M., & Dimitrescu, R. (1957). Stratigraphia şi tectonica Munţilor Apuseni (cu privire specială asupra cristalinului şi Mezozoicului). *Analele Romîno-Sovietice, Seria Geologie-Geografie, 2*, 29–42.

Bleahu, M., Lupu, M., Patrulius, D., Bordea, S., Sţefan, A., Panin, S. (1981). The structure of the Apuseni Mountains. In: *Carpatho-Balkan Geological Association, XII Congress (Bucharest, Romania). Guide to Excursion-B3,* Bucharest: Institute of Geology and Geophysics, Guide Book Series, 23, p. 103.

Bortolotti, V., Marroni, M., Nicolae, I., Pandolfi, L., Principi, G., & Saccani, E. (2004). An update of the Jurassic ophiolites and associated calc-alkaline rocks in the South Apuseni Mountains (western Romania). *Ofioliti, 29*(1), 5–18.

Bucur, I., & Săsăran, E. (2005). Micropaleontological assemblages from the Upper Jurassic-Lower Cretaceous deposits of Trascău Mountains and their biostratigraphic significance. *Acta Paleontologica Romaniae, 5*, 27–38.

Ciulavu, M., Mählmann, R. F., Schmid, S. M., Hofmann, H., Seghedi, A., & Frey, M. (2008). Metamorphic evolution of a very low-to low-grade metamorphic core complex (Danubian window) in the South Carpathians. *Geological Society, London, Special Publications, 298*(1), 281–315.

Corrie, S. L., & Kohn, M. J. (2008). Trace-element distributions in silicates during prograde metamorphic reactions: Implications for monazite formation. *Journal of Metamorphic Geology, 26*(4), 451–464.

Csontos, L., & Vörös, A. (2004). Mesozoic plate tectonic reconstruction of the Carpathian region. *Palaeogeography, Palaeoclimatology, Palaeoecology, 210*(1), 1–56.

Culshaw, N., Mosonyi, E., & Reynolds, P. (2012). New 40 Ar/39 Ar laser single-grain ages of muscovites from mylonitic schists in the Rodna Mountains, Eastern Carpathians, Romania: Correlations with microstructure. *International Journal of Earth Sciences, 101*(1), 291–306.

Dallmeyer, R. D., Neubauer, F., Handler, R., Fritz, H., Muller, W., Pană, D., & Putiš, M. (1996). Tectonothermal evolution of the internal Alps and Carpathians: Evidence from Ar-40/Ar-39 mineral and whole-rock data. *Eclogae Geologicae Helvetiae, 89*(1), 203–227.

Dallmeyer, R. D., Pană, D. I., Neubauer, F., & Erdmer, P. (1999). Tectonothermal evolution of the Apuseni Mountains, Romania: Resolution of Variscan versus alpine events with $^{40}Ar/^{39}Ar$ ages. *Journal of Geology, 107*(3), 329–352.

Denuţ, I. (1998). Caracterizarea structurii geologice Ţicău cu privire specială asupra petrologiei metamorfitelor. *Ph.D. dissertation*, Universitatea "Babeş-Bolyai" Cluj-Napoca, Romania, p. 198.

Dimitrescu, R. (1963). Asupra şisturilor cristaline din Nord-Vestul Transilvaniei (Outline of the crystalline rocks from NW Transylvania). *Societatea de Sţiinte Naturale şi Geografie din Republica Socialistă România, Comunicări de Geologie, II*, 147–154.

Dimitrescu, R. (1966). Muntele Mare. Studiu geologic şi petrografic. *Anuarul Comitetului de Stat al Geologiei, XXXV*, 165–258.

Dimitrescu, R. (1994). Les schistes cristallines des séries de Biharia et de Muncel dans le Bihor Méridional. *Romanian Journal of Petrology, 76*, 159–165.

Dutch, R., & Hand, M. (2010). Retention of Sm–Nd isotopic ages in garnets subjected to high-grade thermal reworking: implications for diffusion rates of major and rare earth elements and the Sm–Nd closure temperature in garnet. *Contributions to Mineralogy and Petrology, 159*(1), 93–112.

Erak, D., Matenco, L., Toljić, M., Stojadinović, U., Andriessen, P. A. M., Willingshofer, E., & Ducea, M. (2016). From nappe stacking to extensional detachments at the contact between the Carpathians and Dinarides—The Jastrebac Mountains of Central Serbia. *Tectonophysics, 710*, 162–183.

Finger, F., Broska, I., Roberts, M. P., & Schermaier, A. (1998). Replacement of primary monazite by apatite-allanite-epidote coronas in an amphibolite facies granite gneiss from the eastern Alps. *American Mineralogist, 83*(3–4), 248–258.

Finger, F., Krenn, E., Schulz, B., Harlov, D., & Schiller, D. (2016). Satellite monazites in polymetamorphic basement rocks of the Alps: Their origin and petrological significance. *American Mineralogist, 101*(5), 1094–1103.

Froitzheim, N., Plašienka, D., & Schuster, R. (2008). Alpine tectonics of the Alps and Western Carpathians. In: McCann, T. (Ed.), *The Geology of Central Europe* (Vol. 2, pp. 1141–1232). London: Geological Society.

Gallhofer, D., von Quadt, A., Schmid, S. M., Guillong, M., Peytcheva, I., & Seghedi, I. (2017). Magmatic and tectonic history of Jurassic ophiolites and associated granitoids from the South Apuseni Mountains (Romania). *Swiss Journal of Geosciences, 110*, 699–719.

Gröger, H. (2006). Thermal and structural evolution of the East Carpathians in northern Romania: from Cretaceous orogeny to final exhumation during Miocene collision. *Ph.D. dissertation*, University Basel, Switzerland, p. 132.

Gröger, H., Fügenschuh, B., Tischler, M., Schmid, S., & Foeken, J. (2008). Tertiary cooling and exhumation history in the Maramures area (internal eastern Carpathians, northern Romania): thermochronology and structural data. *Geological Society, London, Special Publications, 298*(1), 169–195.

Gröger, H., Tischler, M., Fügenschuh, B., & Schmid, S. (2013). Thermal history of Maramureş: Cretaceous metamorphism and exhumation (N Romania). *Geologica Carpathica, 64*(5), 383–398.

Haas, J. (2013). *Geology of Hungary*. Berlin: Regional Geology Reviews, Springer Science., 246 p.

Haas, J., Budai, T. (2014). Geology of the pre-Cenozoic basement of Hungary. *Explanatory Notes for pre-Cenozoic Geological Map of Hungary* (1:500.000). Geological and Geophysical Institute of Hungary, Budapest, Hungary.

Haas, J., Kovács, S., Krystyn, L., & Lein, R. (1995). Significance of Late Permian Triassic facies zones in terrane reconstructions in the Alpine-North Pannonian domain. *Tectonophysics, 242*(1–2), 19–40.

Haas, J., & Péró, C. (2004). Mesozoic evolution of the Tisza Mega-unit. *International Journal of Earth Sciences, 93*, 297–313.

Hârtopanu, I., & Hârtopanu, P. (1986). Intersecting Isogrades—a possible way to find out the polymetamorphism. An Example: The Someş Series. *Dări de Seama ale Sedintelor-Institutul de Geologie si Geofizică, 70–71*(5), 291–299.

Hârtopanu, I., Hârtopanu, P., Balintoni, I., Borcoş, M., Lupu, M., Rusu, A. (1982). Foaia Valea Ierii, *Harta Geologică a României, sc. 1:50.000*. Bucureşti: Institutul de Geologie şi Geofizică.

Henry, D. J., & Guidotti, C. V. (2002). Titanium in biotite from metapelitic rocks: Temperature effects, crystal-chemical controls, and petrologic applications. *American Mineralogist, 87*(4), 375–382.

Henry, D. J., Guidotti, C. V., & Thomson, J. A. (2005). The Ti-saturation surface for low-to-medium pressure metapelitic biotites: Implications for geothermometry and Ti-substitution mechanisms. *American Mineralogist, 90*(2–3), 316–328.

Hoinkes, G., Koller, F., Rantitsch, G., Dachs, E., Hoeck, V., Neubauer, F., et al. (1999). Alpine metamorphism of the Eastern Alps. *Schweizerische Mineralogische und Petrographische Mitteilungen, 79*(1), 155–181.

Hölzl, S., Köhler, H., Kröner, A., Jaeckel, P., & Liew, T. (1991). *Geochronology of the Sri Lankan basement* (Vol. 5). Professional Paper: Geological Survey Department of Sri Lanka.

Horváth, P., & Árkai, P. (2002). Pressure-temperature path of metapelites from the Algyő-Ferencszállás area, SE Hungary: thermobarometric constraints from coexisting mineral assemblages and garnet zoning. *Acta Geologica Hungarica, 45*(1), 1–27.

Iancu, V., Berza, T., Seghedi, A., Gheuca, I., & Hann, H. P. (2005). Alpine polyphase tectono-metamorphic evolution of the South Carpathians: A new overview. *Tectonophysics, 410*(14), 337–365.

Ianovici, V., Borcoş, M., Bleahu, M., Patrulius, D., Lupu, M., Dimitrescu, R., Savu, H. (1976). Geology of the Apuseni Mountains. (pp. 631), Bucureşti: Editura Academiei R.S.R.

Janák, M., Froitzheim, N., Lupták, B., Vrabec, M., & Ravna, E. J. K. (2004). First evidence for ultrahigh-pressure metamorphism of eclogites in Pohorje, Slovenia: Tracing deep continental subduction in the Eastern Alps. *Tectonics, 23*(5), 10. https://doi.org/10.1029/2004tc001641.

Janák, M., Froitzheim, N., Yoshida, K., Sasinková, V., Nosko, M., Kobayashi, T., et al. (2015). Diamond in metasedimentary crustal rocks from Pohorje, Eastern Alps: a window to deep continental subduction. *Journal of Metamorphic Geology, 33*(5), 495–512.

Janots, E., Brunet, F., Goffé, B., Poinssot, C., Burchard, M., & Cemič, L. (2007). Thermochemistry of monazite-(La) and dissakisite-(La): implications for monazite and allanite stability in metapelites. *Contributions to Mineralogy and Petrology, 154*(1), 1–14. https://doi.org/10.1007/s00410-006-0176-2.

Janots, E., Engi, M., Berger, A., Allaz, J., Schwarz, J. O., & Spandler, C. (2008). Prograde metamorphic sequence of REE minerals in pelitic rocks of the Central Alps: implications for allanite–monazite–xenotime phase relations from 250 to 610°C. *Journal of Metamorphic Geology, 26*(5), 509–526.

Jeřábek, P., Lexa, O., Schulmann, K., & Plašienka, D. (2012). Inverse ductile thinning via lower crustal flow and fold-induced doming in the West Carpathian Eo-Alpine collisional wedge. *Tectonics, 31*, 5. https://doi.org/10.1029/2012tc003097.

Kalmár, J. (1994). Outlines of geology of the metamorphic basement of the Sălaj (Szilágy) Basin, Romania. *Acta Geologica Hungarica, 37,* 3–4.

Kalmár, J. (1996). A Szilágysomlyói Măgura (Măgura Şimleului, România) földtani felépítése. *Földtani Közlöny, 126,* 41-65.

Kalmár, J., & Kovács-Pálffy, P. (1996). The Ţicău Hills (NW Transylvanie-Rumania) lithostratigraphy and petrology of the metamorphic rocks. *Geologica Carpathica, 47*, 239–244.

Kohn, M. J., & Malloy, M. A. (2004). Formation of monazite via prograde metamorphic reactions among common silicates: implications for age determinations. *Geochimica et Cosmochimica Acta, 68*(1), 101–113.

Koroknai, B., Horváth, P., Balogh, K., & Dunkl, I. (2001). Alpine metamorphic evolution and cooling history of the Veporic basement in northern Hungary: new petrological and geochronological constraints. *International Journal of Earth Sciences, 90*(3), 740–751.

Kounov, A., & Schmid, S. (2013). Fission-track constraints on the thermal and tectonic evolution of the Apuseni Mountains (Romania). *International Journal of Earth Sciences, 102*, 207–233.

Kounov, A., Seward, D., Burg, J. P., Bernoulli, D., Ivanov, Z., & Handler, R. (2010). Geochronological and structural constraints on the Cretaceous thermotectonic evolution of the Kraishte zone, western Bulgaria. *Tectonics, 29*, 2. https://doi.org/10.1029/2009tc002509.

Kräutner, H. G., Kräutner, F., Tănăsescu, A., & Neacşu, V. (1976). Interprétation des âges radiométriques K/Ar pour les roches métamorphiques régénérées. Un exemple-les Carpates orientales. *Anuarul Institutului de Geologie si Geofizică, 50*, 167–229.

Krenn, E., & Finger, F. (2007). Formation of monazite and rhabdophane at the expense of allanite during Alpine low temperature retrogression of metapelitic basement rocks from Crete, Greece: Microprobe data and geochronological implications. *Lithos, 95*(1), 130–147.

Lelkes-Felvári, G., Árkai, P., Sassi, F. P., & Balogh, K. (1996). Main features of the regional metamorphic events in Hungary: A review. *Geologica Carpathica, 47*(4), 257–270.

Lelkes-Felvári, G., Frank, W., & Schuster, R. (2003). Geochronological constraints of the Variscan, Permian-Triassic and eo-Alpine (Cretaceous) evolution of the Great Hungarian Plain basement. *Geologica Carpathica, 54*(5), 299–316.

Lelkes-Felvári, G., Mazzoli, C., & Visona, D. (1989). Contrasting mineral assemblages in polymetamorphic rocks from South Transdanubia (Hungary). *European Journal of Mineralogy, 1*, 143–146.

Lelkes-Felvári, G., Schuster, R., Frank, W., & Sassi, R. (2005). Metamorphic history of the Algyő High (Tisza Mega-unit, basement of Great Hungarian Plain)—a counterpart of crystalline units of the Koralpe-Wölz nappe system (Austroalpine, Eastern Alps). *Acta Geologica Hungarica, 48*(4), 371–394.

Lorinczi, P., & Houseman, G. (2010). Geodynamical models of lithospheric deformation, rotation and extension of the Pannonian Basin of Central Europe. *Tectonophysics, 492*(1–4), 73–87.

Ludwig, K. (2012). User manual for Isoplot version 3.75–4.15: a geochronological toolkit for Microsoft Excel. *Berkley Geochronological Center Special Publication,* 5, p. 75, http://bgc.org/isoplot_etc/isoplot/Isoplot3_75-4_15manual.pdf

Márton, E. (2000). The Tisza Megatectonic Unit in the light of palaeomagnetic data. *Acta Geologica Hungarica, 43*, 329–343.

Márton, E., & Fodor, L. (2003). Tertiary paleomagnetic results and structural analysis from the Transdanubian Range (Hungary): rotational disintegration of the Alcapa unit. *Tectonophysics, 363*, 201–224.

Márton, E., Tischler, M., Csontos, L., Fügenschuh, B., & Schmid, S. M. (2007). The contact zone between the ALCAPA and Tisza-Dacia megatectonic units of Northern Romania in the light of new paleomagnetic data. *Swiss Journal of Geosciences*, *100*(1), 109–124.

Mârza, I. (1965). Unitatea Petrografică şi Paleostratigrafică a masivelor de carbonaţi metamorfici: Vulturese-Scărişoara-Leurda (Bazinul Arieşului). *Analele Universităţii Bucureşti: Seria ştiinţele naturii Geologie-Geografie, 14*, 9–17.

Mârza, I. (1969). *Evoluţia unităţilor cristaline din sud-estul Muntelui Mare.* Bucharest: Editura Academiei Republicii Socialiste România, 1

McCulloch, M., & Wasserburg, G. (1978). Sm–Nd and Rb–Sr Chronology of Continental Crust Formation. *Science, 200*(4345), 1003–1011.

Mezger, K., Essene, E., & Halliday, A. (1992). Closure temperatures of the Sm-Nd system in metamorphic garnets. *Earth and Planetary Science Letters, 113*(3), 397–409.

Mosonyi, E. (1999). Geological and structural studies on metamorphics from the southern part of Rodna Mountains (East Carpathians). *Ph.D. dissertation*, University Babeş-Bolyai, Cluj-Napoca, Romania, p. 276.

Mosonyi, E., & Kristály, F. (2014). A Possible Permo-Triassic Thermo-Tectonic Event in Rodna Mts (East Carpathians, Romania). *Buletini i Shkencave Gjeologjike, Special Issue, 1*, 205–208.

Munteanu, M., & Tatu, M. (2003). The East-Carpathian crystalline-mesozoic zone (Romania): paleozoic amalgamation of Gondwana-and East European craton derived terranes. *Gondwana Research, 6*(2), 185–196.

Necea, D. (2010). High-resolution morpho-tectonic profiling across an orogen: tectonic-controlled geomorphology and multiple dating approach in the SE Carpathians. *Ph.D. dissertation*, ISBN 9789086594320, Vrije Universiteit, Amsterdam, Netherlands, p. 147.

Negulescu, E., Săbău, G., & Massonne, H. J. (2018). Growth of chloritoid and garnet along a nearly isothermal burial path to 70 km depth: an example from the Bughea Metamorphic Complex, Leaota Massif, South Carpathians. *Mineralogy and Petrology, 112*(4), 535-553. https://doi.org/10.1007/s00710-017-0552-9.

Nicolae, I., Soroiu, M., & Bonhomme, G. (1992). Ages K-Ar de quelques ophiolites des Monts Apuseni du sud (Roumanie) et leur signification géologique. *Géologie Alpine, 68*, 77–83.

Pană, D., & Balintoni, I. (2000). Igneous protoliths of the Biharia lithotectonic assemblage: timing of intrusion, geochemical consideration, tectonic setting. *Studia Universitatis Babeş-Bolyai, Geologia, 45*(1), 3–22.

Pană, D. I., Heaman, L. M., Creaser, R. A., & Erdmer, P. (2002). Pre-alpine crust in the Apuseni Mountains, Romania: Insights from Sm-Nd and U-Pb data. *Journal of Geology, 110*(3), 341–354.

Pătraşcu, S., Panaiotu, C., Seşclăman, M., & Panaiotu, C. E. (1994). Timing of rotational motion of Apuseni mountains (Romania): paleomagnetic data from Tertiary magmatic rocks. *Tectonophysics, 233*, 163–176.

Pavelescu, L., Pop, G., Ailenei, G., Ene, I., Soroiu, M., & Popescu, G. (1975). K-Ar age determinations from the Apuseni and Banat Mountains. *Revue Roumaine de Géologie, Géophysique et Géographie, 19*, 67–69.

Pozsgai, E., Józsa, S., Dunkl, I., Sebe, K., Thamó-Bozsó, E., Sajó, I., et al. (2017). Provenance of the Upper Triassic siliciclastics of the Mecsek Mountains and Villány Hills (Pannonian Basin, Hungary): constraints to the early Mesozoic paleogeography of the Tisza Megaunit. *International Journal of Earth Sciences, 106*(6), 2005–2024.

Pyle, J. M., Spear, F. S., Cheney, J. T., & Layne, G. (2005). Monazite ages in the Chesham Pond Nappe, SW New Hampshire, USA: Implications for assembly of central New England thrust sheets. *American Mineralogist, 90*(4), 592–606.

Radu, D. (1997). Geothermometry of metapelitic rocks from the western part of Preluca crystalline complex, Maramureş. *Romanian Journal of Mineralogy, 78*, 21–30.

Radu, D. (2003). Evoluia termobarică a rocilor metamorfice din masivele Preluca, Ţicău şi Codru, NV Transilvaniei. *Ph.D. dissertation*, Bucharest University, Romania, p. 222.

Reiser, M. K. (2015). The tectonometamorphic evolution of the Apuseni Mountains during the Cretaceous. *Ph.D. dissertation*, urn:nbn:at:at-ubi:1-2287, University of Innsbruck, Austria, p. 168.

Reiser, M. K., Schuster, R., Spikings, R., Tropper, P., & Fügenschuh, B. (2017a). From nappe stacking to exhumation: Cretaceous tectonics in the Apuseni Mountains (Romania). *International Journal of Earth Sciences, 106*, 659–685.

Reiser, M. K., Schuster, R., Tropper, P., & Fügenschuh, B. (2017b). Constraints on the depositional age and tectonometamorphic evolution of marbles from the Biharia Nappe System (Apuseni Mountains, Romania). *Geologica Carpathica, 68*(2), 147–164.

Săndulescu, M. (1984). *Geotectonics of Romania* (p. 343). Bucharest: Editura Tehnică.

Schmid, S. M., Bernoulli, D., Fügenschuh, B., Matenco, L., Schefer, S., Schuster, R., et al. (2008). The Alpine-Carpathian-Dinaridic orogenic system: correlation and evolution of tectonic units. *Swiss Journal of Geosciences, 101*(1), 139–183.

Schuller, V. (2004). Evolution and geodynamic significance of the Upper Cretaceous Gosau basin in the Apuseni Mountains (Romania). *Ph.D. dissertation*, Tübinger geowissenschaftliche Arbeiten Reihe A70, Universität Tübingen, Germany, p. 122.

Schuller, V., Frisch, W., Danisik, M., Dunkl, I., & Melinte, M. C. (2009). Upper Cretaceous Gosau Deposits of the Apuseni Mountains (Romania)—similarities and differences to the Eastern Alps. *Austrian Journal of Earth Sciences, 102*(1), 133–145.

Schulz, B. (2016). Polymetamorphism in garnet micaschists of the Saualpe Eclogite Unit (Eastern Alps, Austria), resolved by automated SEM methods and EMP–Th–U–Pb monazite dating. *Journal of Metamorphic Geology, 35*(2), 141–163.

Schuster, R., Koller, F., Hoeck, V., Hoinkes, G., & Bousquet, R. (2004). Explanatory notes to the map: metamorphic structure of the Alps-Metamorphic evolution of the Eastern Alps. *Mitteilungen der Österreichischen Mineralogischen Gesellschaft, 149*, 175–199.

Schuster, R., & Stüwe, K. (2008). Permian metamorphic event in the Alps. *Geology, 36*(8), 603–606.

Schuster, R., Tropper, P., Krenn, E., Finger, F., Frank, W., & Philippitsch, R. (2015). Prograde Permo-Triassic metamorphic HT/LP assemblages from the Austroalpine Jenig Complex (Carinthia, Austria). *Austrian Journal of Earth Sciences, 108*(1), 73–90.

Smith, H. A., & Barreiro, B. (1990). Monazite U-Pb dating of staurolite grade metamorphism in pelitic schists. *Contributions to Mineralogy and Petrology*, *105*(5), 602–615.

Soroiu, M., Balintoni, I., & Vodă, A. (1985). A model of the basement of the Transylvanian Basin as revealed by K-Ar dating. *Revue Roumaine de Géologie, Géophysique et Géographie, 29*, 29–35.

Spear, F. S. (2010). Monazite-allanite phase relations in metapelites. *Chemical Geology, 279*(1), 55–62.

Spear, F. S., & Pyle, J. M. (2010). Theoretical modeling of monazite growth in a low-Ca metapelite. *Chemical Geology, 273*(1–2), 111–119.

Strutinski, C., Puşte, A., & Stan, R. (2006). The metamorphic basement of Romanian Carpathians: a discussion of K-Ar and 40Ar/39Ar ages. *Studia Universitatis Babe-Bolyai, Geologia, 51*(1–2), 15–21.

Szederkényi, T., Haas, J., Nagymarosy, A., & Hámor, G. (2012). Geology and History of Evolution of the Tisza Mega-Unit. In J. Haas (Ed.), *Geology of Hungary* (pp. 103–148). Berlin, Heidelberg: Springer Science.

Thomsen, T. B., Heijboer, T., & Guarnieri, P. (2016). jAgeDisplay: software for evaluation of data distributions in U-Th-Pb geochronology. *Geological Survey of Denmark and Greenland Bulletin, 35*, 103–106.

Thöni, M. (2002). Sm-Nd isotope systematics in garnet from different lithologies (Eastern Alps): age results, and an evaluation of potential problems for garnet Sm–Nd chronometry. *Chemical Geology, 185*(3), 255–281.

Thöni, M., & Miller, C. (2009). The Permian event in the Eastern European Alps: Sm–Nd and P-T data recorded by multi-stage garnet from the Plankogel unit. *Chemical Geology, 260*(1–2), 20–36.

Thöni, M., Miller, C., Zanetti, A., Habler, G., & Goessler, W. (2008). Sm-Nd isotope systematics of high-REE accessory minerals and major phases: ID-TIMS, LA-ICPMS and EPMA data constrain multiple Permian-Triassic pegmatite emplacement in the Koralpe, Eastern Alps. *Chemical Geology, 254*(3), 216–237.

Tischler, M., Gröger, H., Fügenschuh, B., & Schmid, S. (2007). Miocene tectonics of the Maramures area (Northern Romania): implications for the Mid-Hungarian fault zone. *International Journal of Earth Sciences, 96*(3), 473–496.

Tischler, M., Matenco, L., Filipescu, S., Gröger, H. R., Wetzel, A., & Fügenschuh, B. (2008). Tectonics and sedimentation during convergence of the ALCAPA and Tisza-Dacia continental blocks: The Pienide nappe emplacement and its foredeep (N. Romania). *Geological Society, London, Special Publications, 298*(1), 317–334.

Tuccillo, M., Essene, E., & Van Der Pluijm, B. (1990). Growth and retrograde zoning in garnets from high-grade, metapelites: Implications for pressure-temperature paths. *Geology, 18*(9), 839–842.

Udubaşa, G., Hârtopanu, P., Ilinca, G., & Valdman, S. (1996). The regionally metamorphosed Mn-Fe deposit at Răzoare, Preluca Mts., Romania. *Romanian Journal of Mineral Deposits, 77*, 3–20.

Ustaszewski, K., Schmid, S. M., Fügenschuh, B., Tischler, M., Kissling, E., & Spakman, W. (2008). A map-view restoration of the Alpine-Carpathian-Dinaridic system for the Early Miocene. *Swiss Journal of Geosciences, 101*(1), 273–294.

van Gelder, I., Matenco, L., Willingshofer, E., Tomljenović, B., Andriessen, P. A. M., Ducea, M., et al. (2015). The tectonic evolution of a critical segment of the Dinarides-Alps connection: Kinematic and geochronological inferences from the Medvednica Mountains, NE Croatia. *Tectonics, 34*, 1952–1978.

Vojtko, R., Králiková, S., Andriessen, P., Prokešová, R., Minár, J., & Jěrábek, P. (2017). Geological evolution of the southwestern part of the Veporic Unit (Western Carpathians): based on fission track and morphotectonic data. *Geologica Carpathica, 68*(4), 285–302.

Vojtko, R., Králiková, S., Jěrábek, P., Schuster, R., Danišík, M., Fügenschuh, B., et al. (2016). Geochronological evidence for the Alpine tectono-thermal evolution of the Veporic Unit (Western Carpathians, Slovakia). *Tectonophysics, 666*, 48–65.

Whitney, D., & Evans, B. (2010). Abbreviations for names of rock-forming minerals. *American Mineralogist, 95*(1), 185.

Wing, B. A., Ferry, J. M., & Harrison, T. M. (2003). Prograde destruction and formation of monazite and allanite during contact and regional metamorphism of pelites: petrology and geochronology. *Contributions to Mineralogy and Petrology, 145*(2), 228–250.

Zimmerman, A., Stein, H. J., Hannah, J. L., Kozelj, D., Bogdanov, K., & Berza, T. (2008). Tectonic configuration of the Apuseni-Banat-Timok-Srednogorie belt, Balkans-South Carpathians, constrained by high precision Re-Os molybdenite ages. *Mineralium Deposita, 43*(1), 1–21.

Zincenco, D., Soroiu, M., & Cuna, S. (1990). Cretaceous thermal front on pre-Mesozoic continental crust, documented by K-Ar data: an example, The Sylvanic belts, NW Transylvania. *Revue Roumaine de Géologie, Géophysique et Géographie, 34*, 95–105.